Studying the Complex Absorption & Emission Lines in AGN spectra

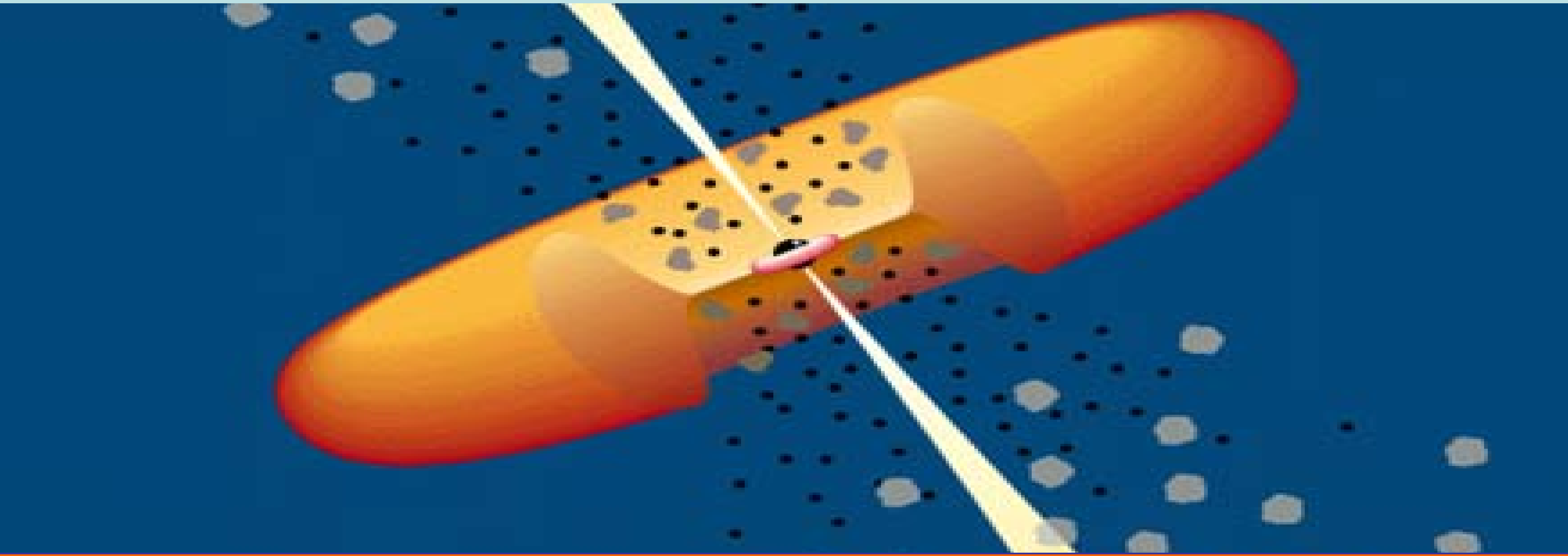

Eleni T. Chatzichristou

Institute of Astronomy & Astrophysics, National Observatory of Athens

E. Danezis *(University of Athens)*, ***L.C. Popovic*** *(Astronomical Observatory of Belgrade)*,
E. Lyratzi *(University of Athens)*, ***M.S. Dimitrijevic*** *(Astronomical Observatory of Belgrade)*

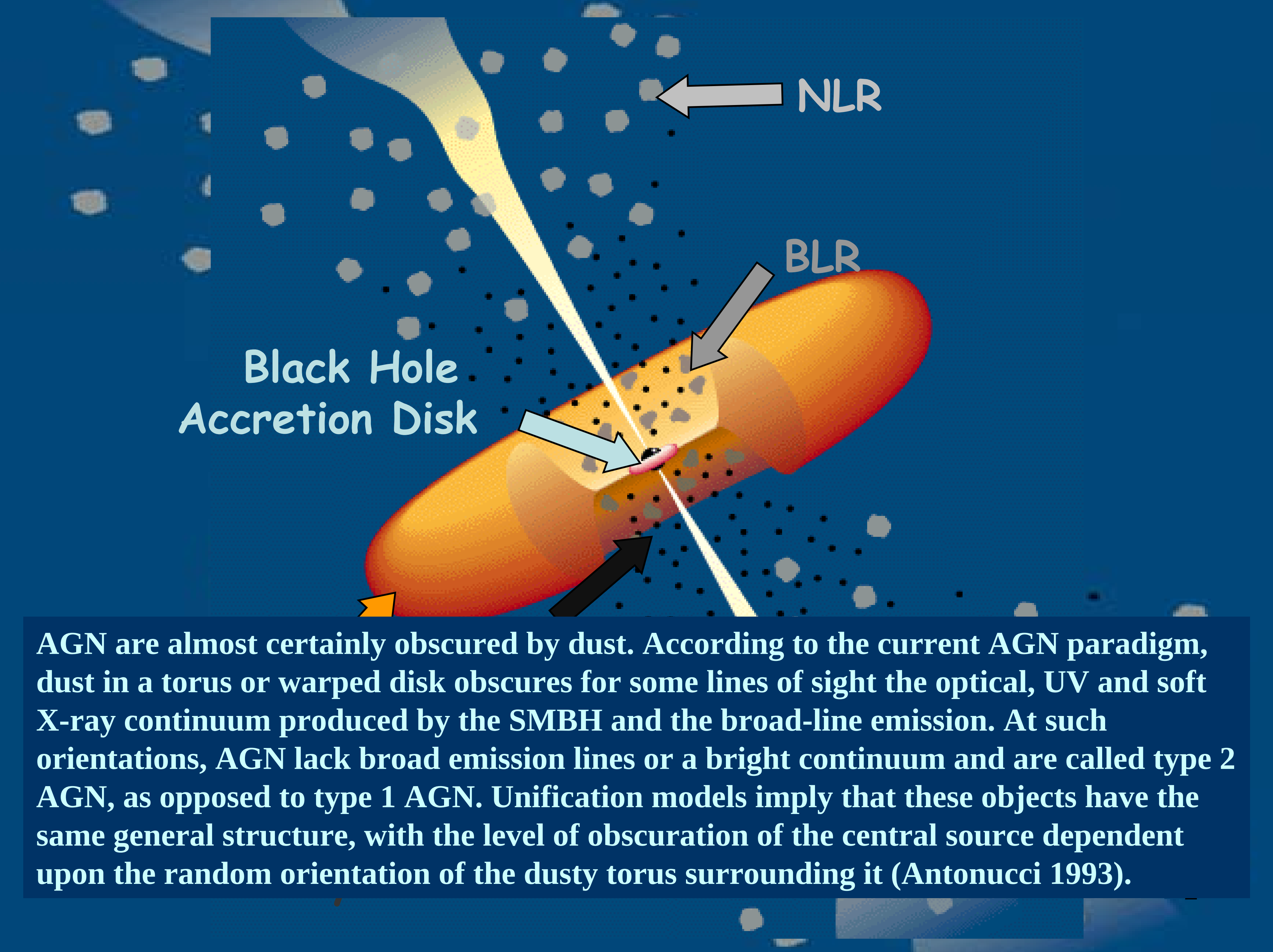

AGN are almost certainly obscured by dust. According to the current AGN paradigm, dust in a torus or warped disk obscures for some lines of sight the optical, UV and soft X-ray continuum produced by the SMBH and the broad-line emission. At such orientations, AGN lack broad emission lines or a bright continuum and are called type 2 AGN, as opposed to type 1 AGN. Unification models imply that these objects have the same general structure, with the level of obscuration of the central source dependent upon the random orientation of the dusty torus surrounding it (Antonucci 1993).

The broad emission lines are formed in a very compact region (**BLR**) confined in the central part of AGN -> information on the condition of the emitting gas surrounding the super-massive black hole.

The physics in the BLR is far more complicated than is in the NLR.
Photoionization the dominant heating mechanism of the BLR emitting gas, although recombination and collisions are also relevant processes.
The kinematics of the BLR (e.g. Sulentic et al. 2000) assuming spherical, cylindrical or disk geometry (e.g. Popović et al. 2004).

It might be that the broad emission lines are produced in two or more kinematically and physically different emission regions, i.e. that multiple emission components with fundamentally different velocity distributions might be present in the spectra.

What is the physical connection between broad emission and absorption lines?

In AGN, mass accretion onto the central SMBH occurs in conjunction with massive outflows. These are believed to be:
(1) Winds driven by radiation and gas pressure from the disk photosphere ($\sim 10^{16}$cm), radially accelerated by UV photons to velocities 0.1-0.3c.
(2) Low-velocity dust-driven winds from AGB stars that orbit around the center, radiatively accelerated by dust absorption.

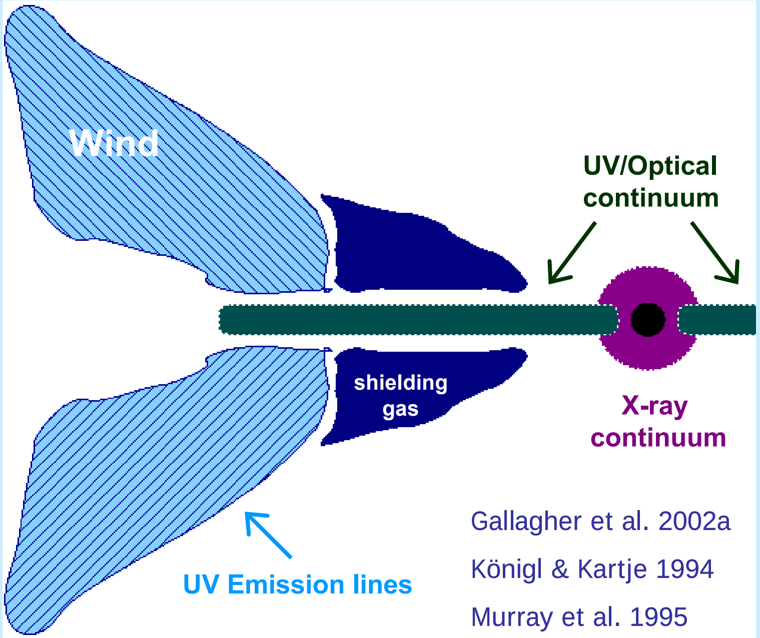

BALs are particularly conspicuous in ~10% of quasars, the so-called **BAL QSOs**, for which the l.o.s is passing through the outflow. BALs are seen in high ionization UV resonance transitions: ***NV (1240A), SiIV (1400A), CIV(1550A)*** and eventually MgII (2800A). Probably the Blue-shifted A lines are due to outflow+obscuration.

Exploring the QSO environment near the central source, within a few-100s pc.
Where are the emission and absorption line regions situated?

- Central continuum source ~10^{17} cm
- Lyα emission ~ 10^{18} cm (anisotropically? from the far-side clouds?)
- BALR further than BELR, covering the central source by <0.2
- NV BAL might cover the Lyα region completely or be closer to the central source
- SiIV & CIV BAL may not completely cover the central source if lie within the BELR
- OVI BAL contaminated by Lya forest lines
- Emission may also be coming from the absorbing clouds
- *BEL and BAL regions could be co-spatial*

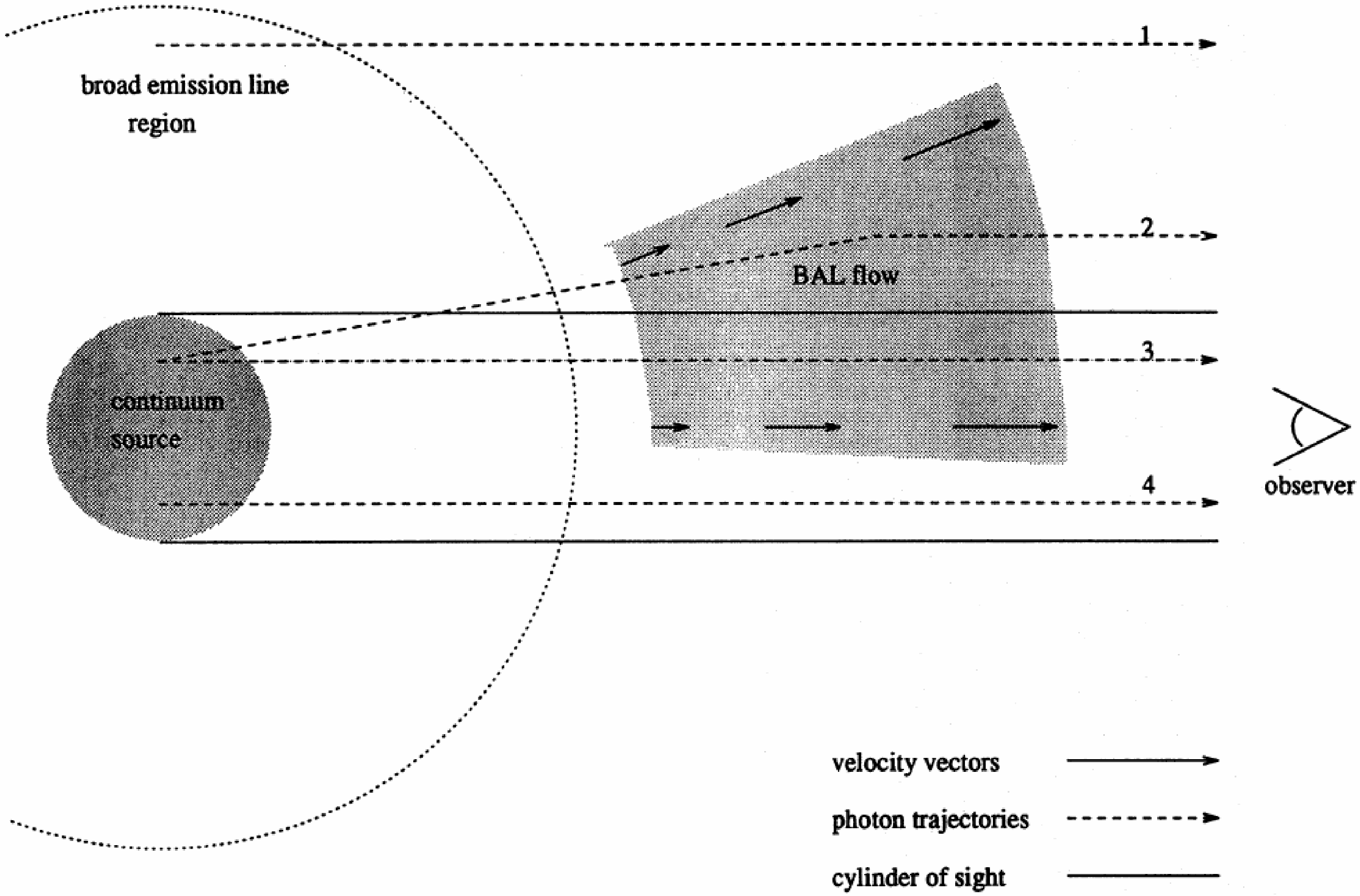

FIG. 5.—Schematic geometry of the BALQSO environment and the four photon trajectories that can reach the observer: (1) photons from parts of the BELR not covered by the BAL flow (as seen by the observer), (2) photons that were scattered by the BAL flow into the line of sight, (3) photons with original direction along the line of sight that passed through the flow but were not scattered, and (4) photons from parts of the continuum source that are not covered by the flow (as seen by the observer).

Arav 1996, ApJ 465, 617

How are the BAL emitted?

- Could be coming from a spatially distinct region (cloud, part of wind) or from more than one regions with large spatial separations.
- The l.o.s. might be intercepting two regions with the same outflow velocity.
- BAL multi-layered structure, spatially distinct with similar densities, or continuous with different densities.

Furthermore, the gas giving rise to BALs might have not a uniform ionization: photoionization by the central source + collisional excitation.

Shape of outflow might be changing according to luminosity of central source

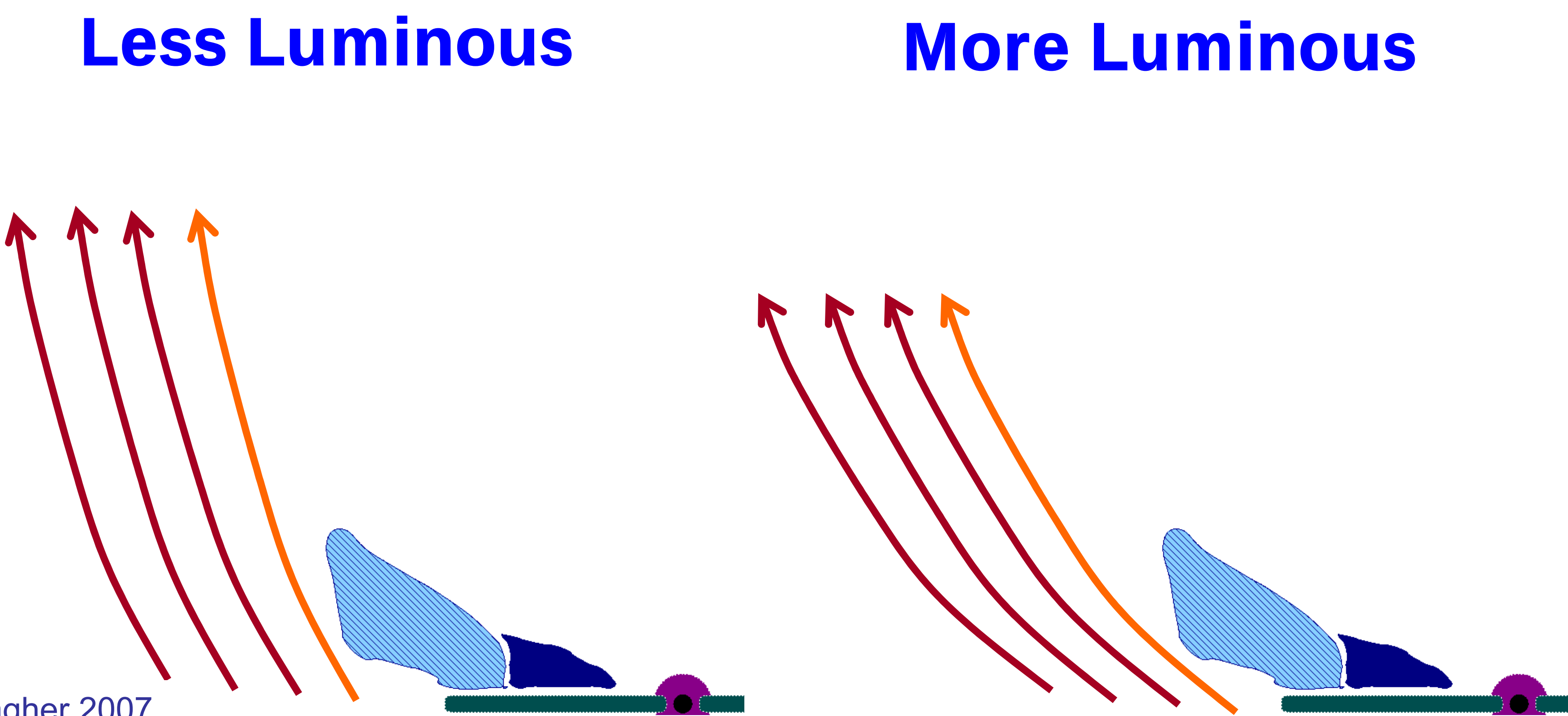

Gallagher 2007

BAL do not start from 0 velocity wrt the corresponding BEL, detached by 10^3 km/s, up to -15000 km/s. Could be due to small non-radial velocity component in the flow. This plus the 3d structure of the flow (multiple and/or curved) could account for the complex BAL shapes, multi-troughs (DACs) and overlapping troughs (SACs).

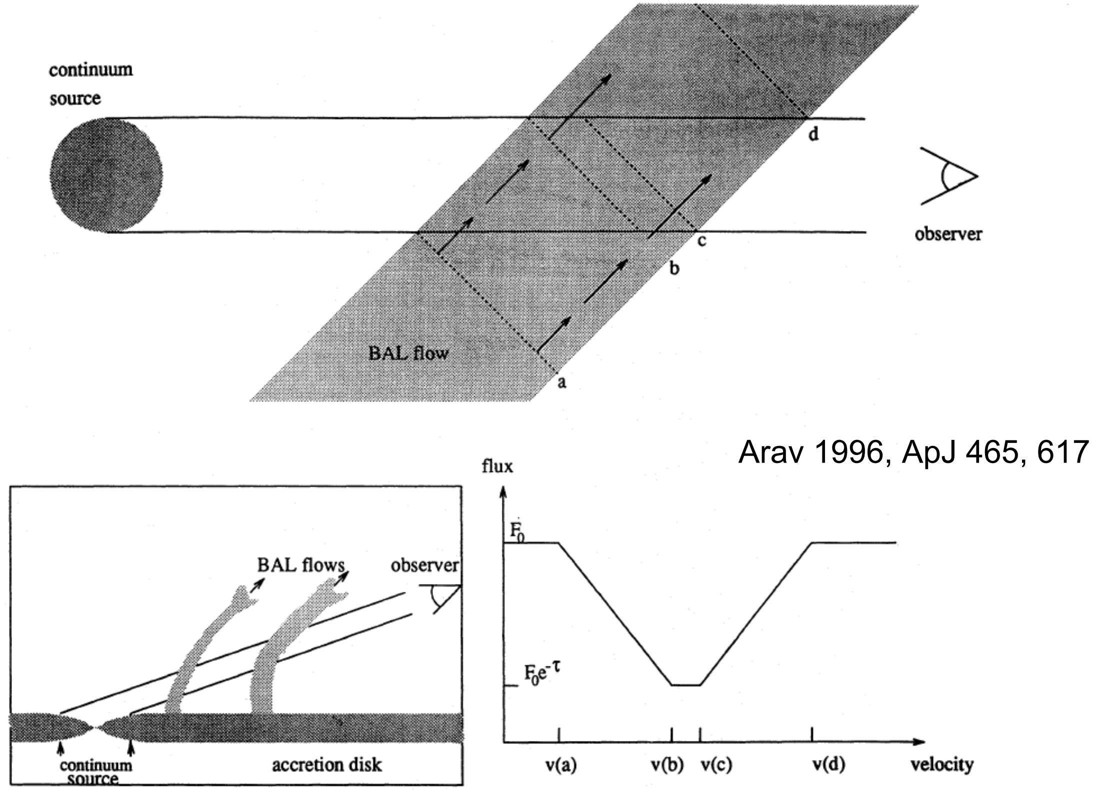

Arav 1996, ApJ 465, 617

FIG. 3.—Illustration of the in and out of line-of-sight effect for the simple case of an accelerating straight BAL flow in two dimensions. The solid lines

Also, the velocity detachment could be due to:
- the episodic nature of the flow (mass ejections/outbursts)
- small clouds from a larger confining flow at the appropriate velocities.

$v_{outflow} \sim (0.03\text{-}0.2)c$

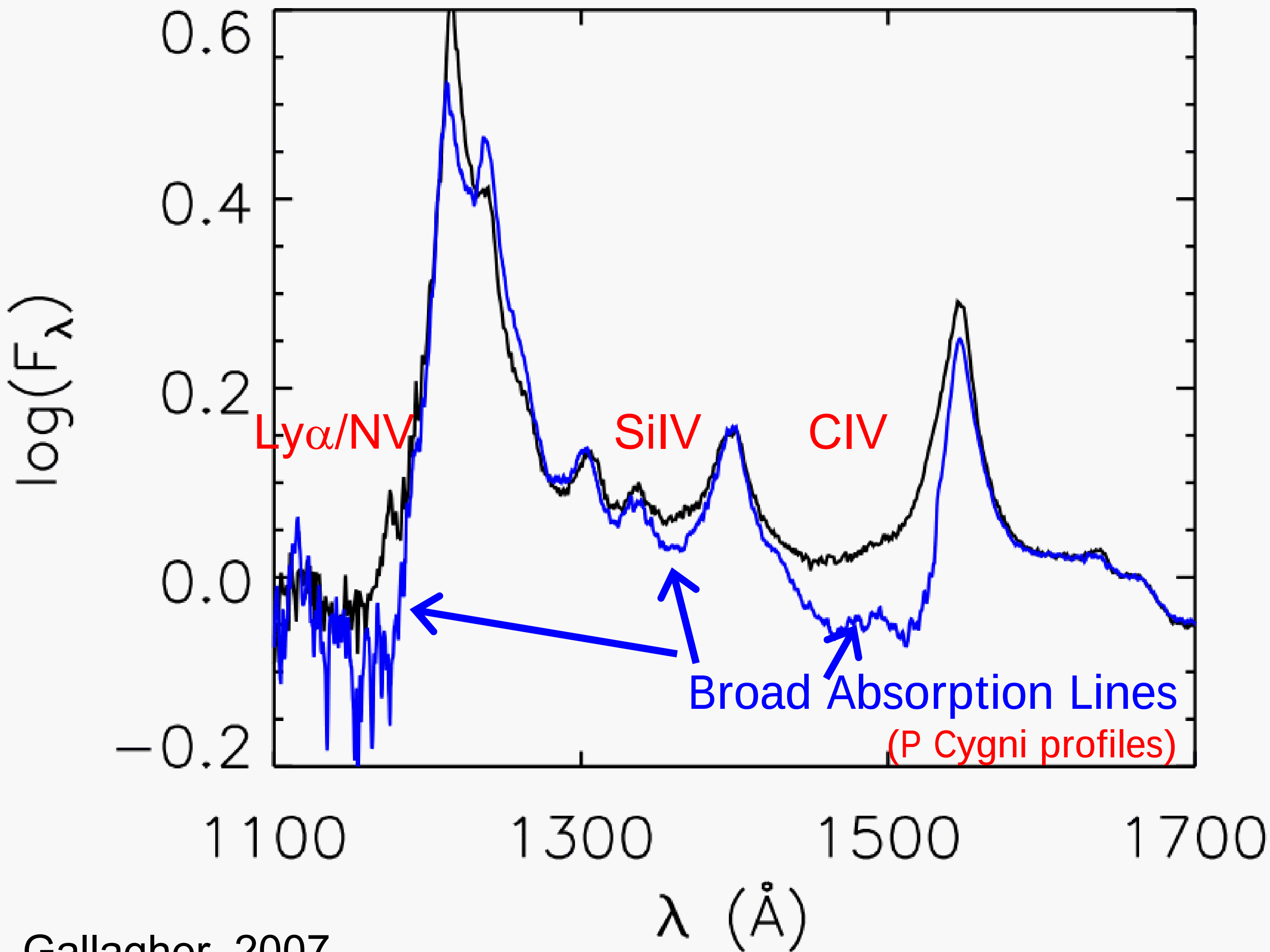

Gallagher, 2007

Lyα “ghost” signature:
If radiative acceleration via resonance line scattering
The accelerating NV ions see a strong change in the Lyα ionizing flux, acceleration increases, optical depth of the wind increases imitating the Lya profile
Lyα peak occurs at -5900 km/s in the rest frame of NV ions.
The effect will occur to the other absorbing ions as well. Most prominent for the CIV BAL (small separation of doublet and smaller than the width of Lyα BEL.

Arav 1996, ApJ 465, 617

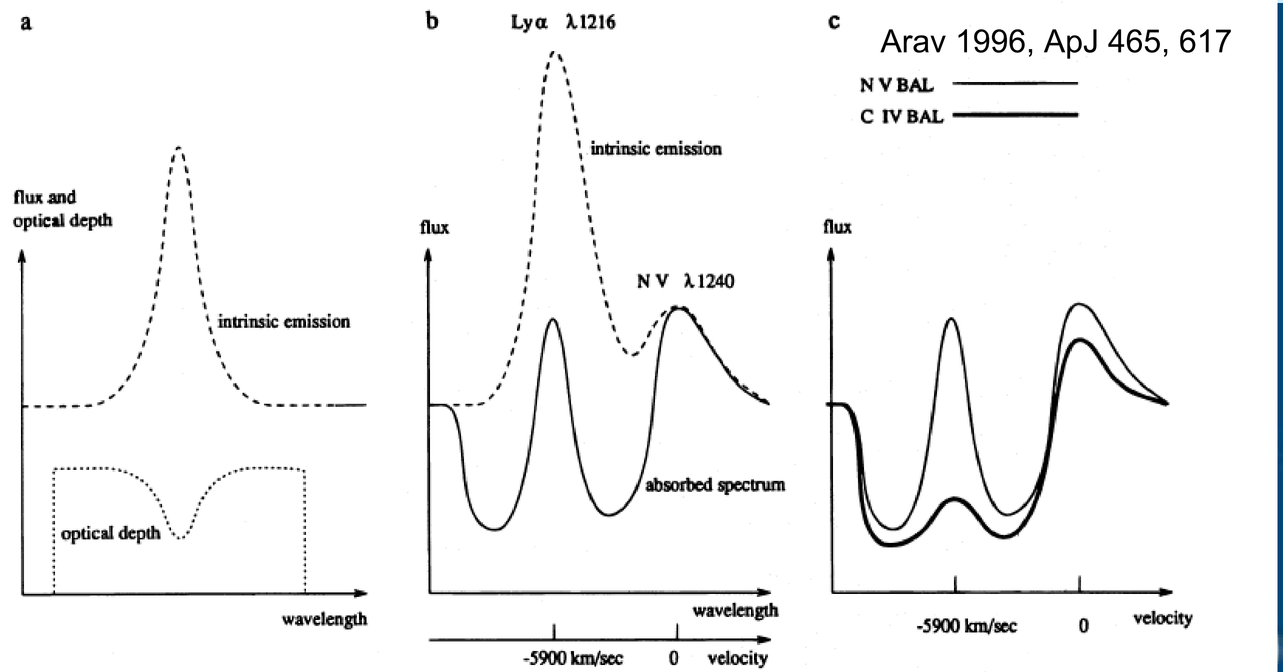

FIG. 1.—Schematic illustration for the creation of the ghost of Lyα signature (based on eq. [A1] in the Appendix; for an overview of the model see § 2). For a constant νL_ν (where ν is frequency and L_ν is the luminosity per unit frequency), pure radiative acceleration creates an absorption trough with a constant optical depth. When the accelerating ions sample an increasing flux, their acceleration, relative to the constant νL_ν case, increases, and as a result the optical depth of the wind decreases. In panel (a) we show the optical depth changes that result from the exposure of the accelerating ions to a strong emission line. A very similar situation is found in quasars; panel (b) shows the spectral regime around a quasar's strongest emission line, Lyα. The N V ions are exposed to the strong Lyα flux, and in their rest frame the peak of Lyα occurs at a velocity of -5900 km s^{-1}. Since we do not know the intrinsic Lyα emission spectrum, it is impossible to determine from the absorbed spectrum whether the optical depth has changed at the appropriate velocity interval. However, the N V ions share their acceleration with the rest of the flow through Coulomb collisions or the presence of magnetic fields, and thus gives the optical depth modulation to all

So the question is whether we see a Lyα ghost or double troughs.

With high resolution, high S/N spectra one could eventually constrain the geometry and kinematics of the flows.

Method:

Model of Danezis et al. (2003):
BAL region is composed by a number of successive independent absorbing density layers, originating in a disk wind, with constant rotational and radial velocities.

- Using pure gaussian profiles (random velocities) and/or rotation, to probe the two extremes. A combination would be a most probable situation, next step :Voigt
- Testing various geometries: BEL closer to the central source than BAL, and cospatial BEL and BAL.
- Test sample of well-observed BAL QSOs (not complete by any means).

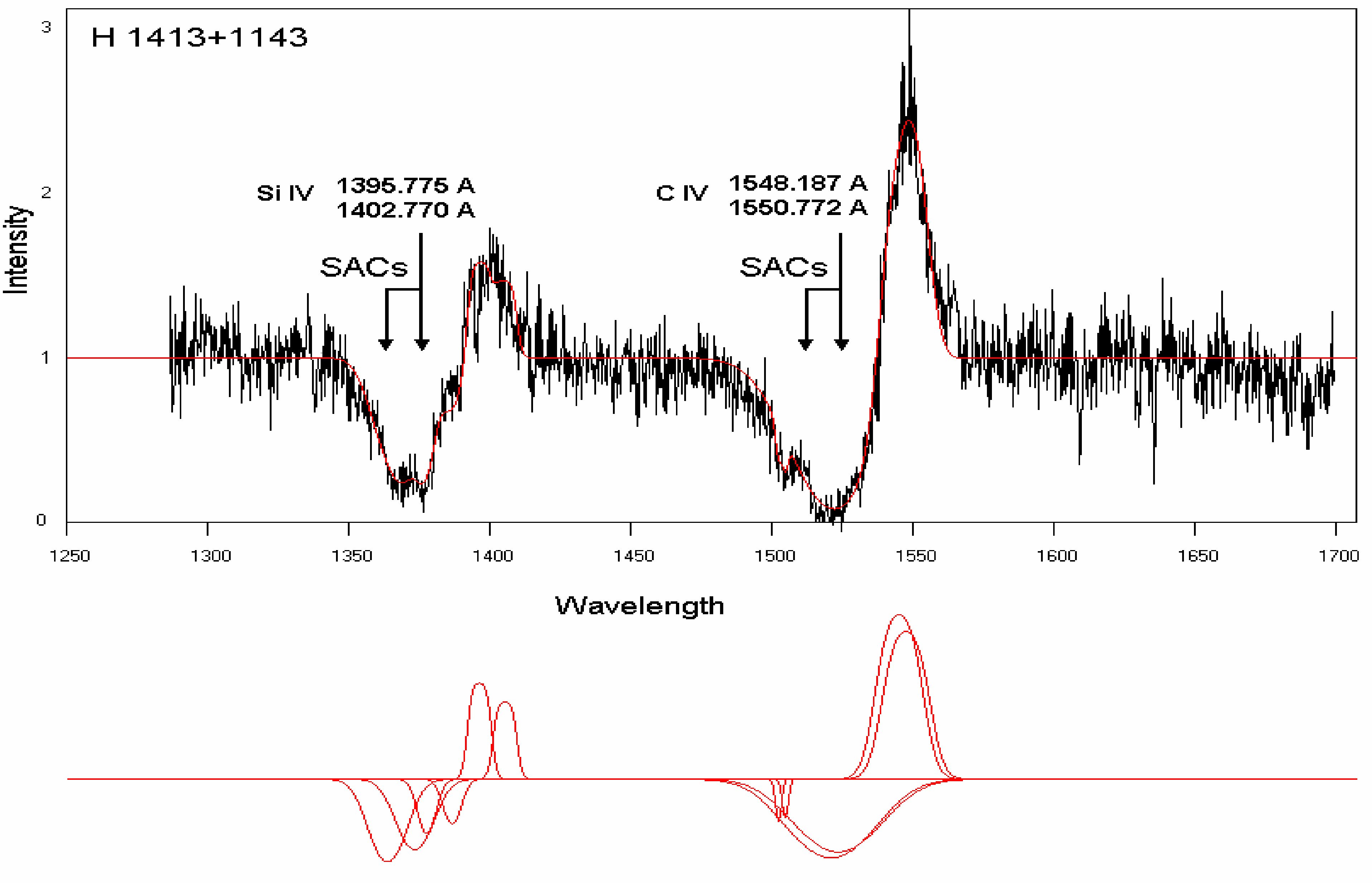

H 1413+1143
Si IV
1395.775 A
1402.770 A
SACs
C IV
1548.187 A
1550.772 A
SACs
Intensity
Wavelength
0
1
2
3
1250
1300
1350
1400
1450
1500
1550
1600
1650
1700

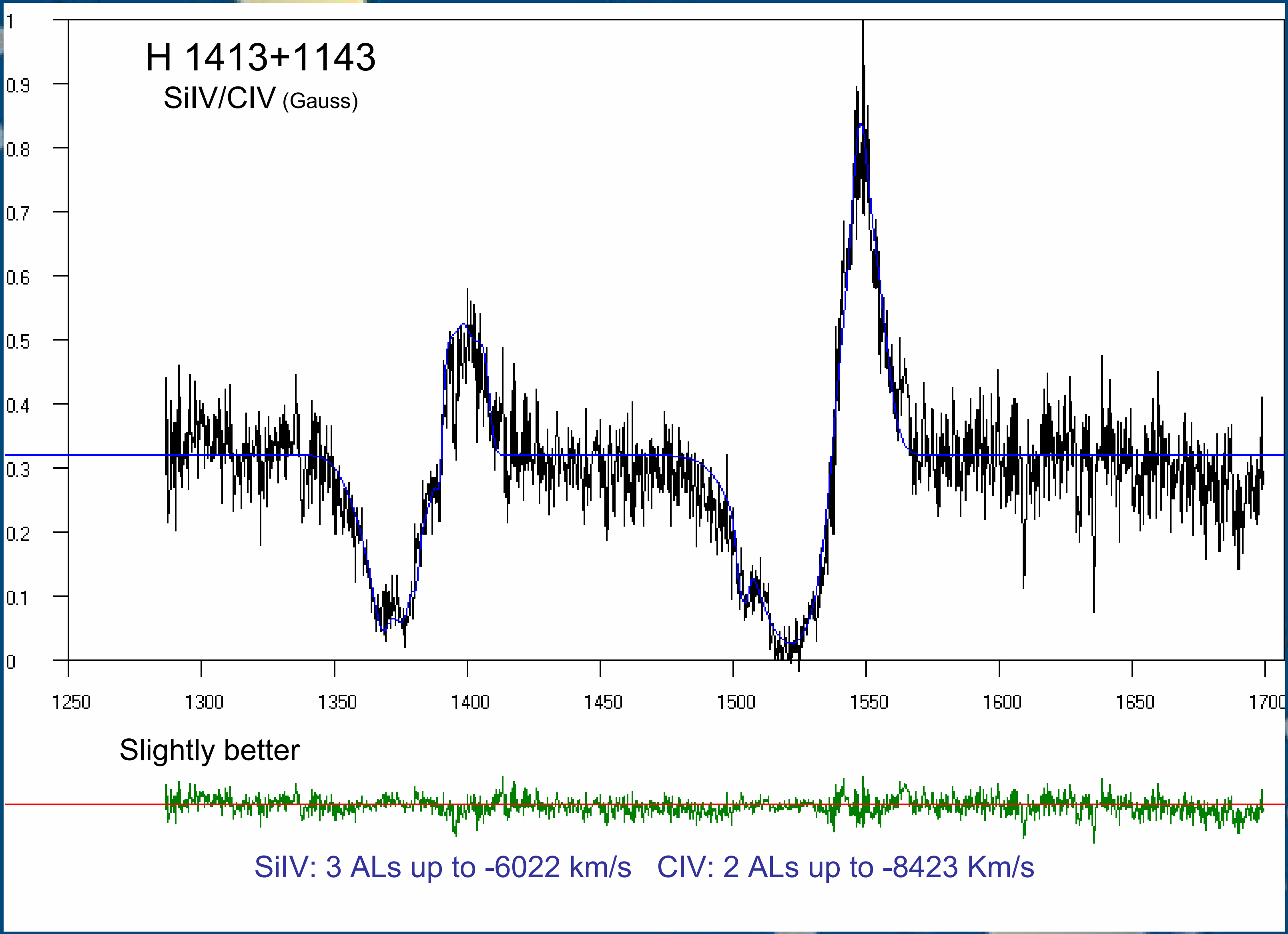
H 1413+1143
SiIV/CIV (Gauss)
1
0.9
0.8
0.7
0.6
0.5
0.4
0.3
0.2
0.1
0
1250
1300
1350
1400
1450
1500
1550
1600
1650
1700
Slightly better
SiIV: 3 ALs up to -6022 km/s CIV: 2 ALs up to -8423 Km/s

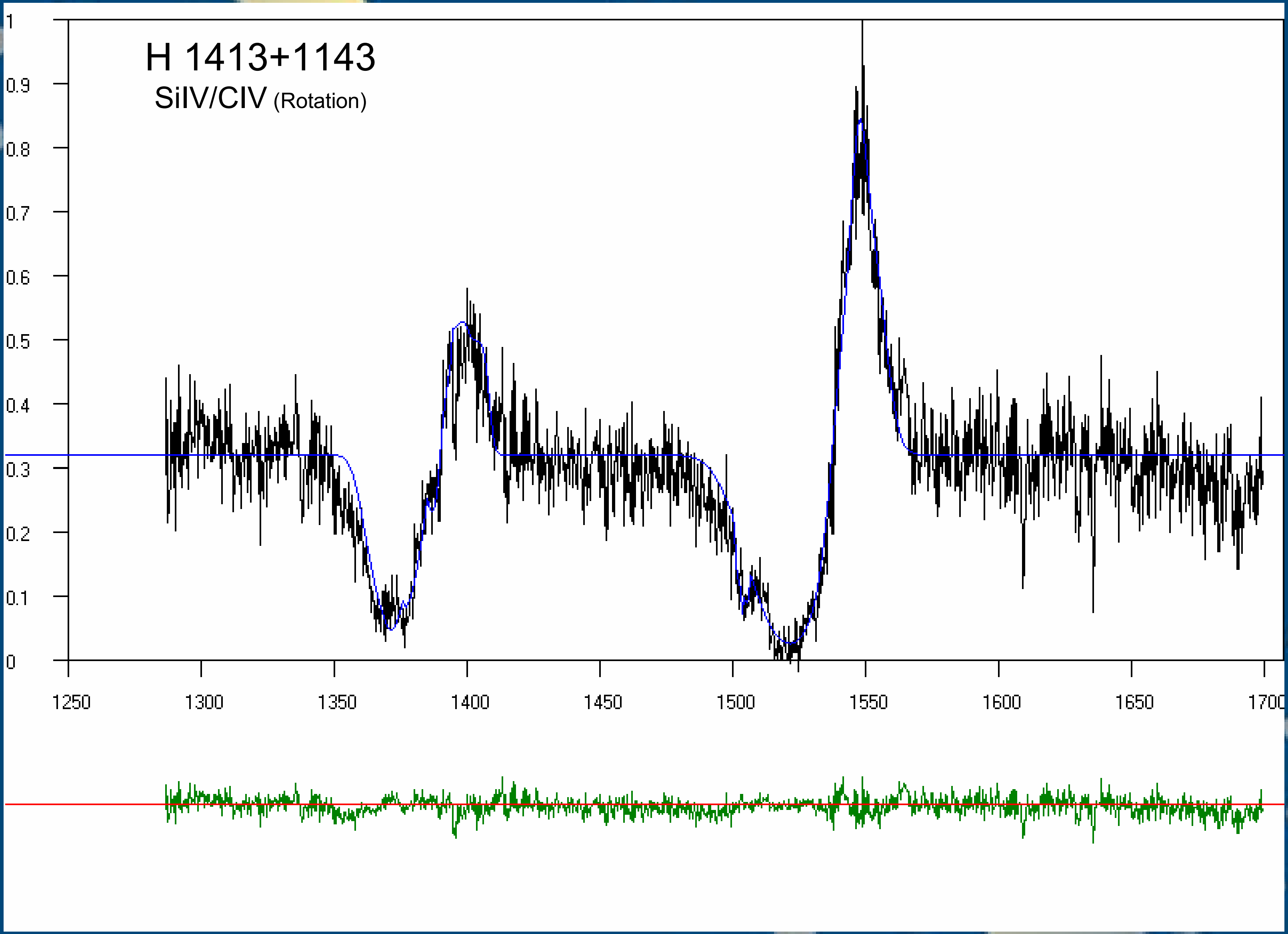
H 1413+1143
SiIV/CIV (Rotation)
1
0.9
0.8
0.7
0.6
0.5
0.4
0.3
0.2
0.1
0
1250
1300
1350
1400
1450
1500
1550
1600
1650
1700

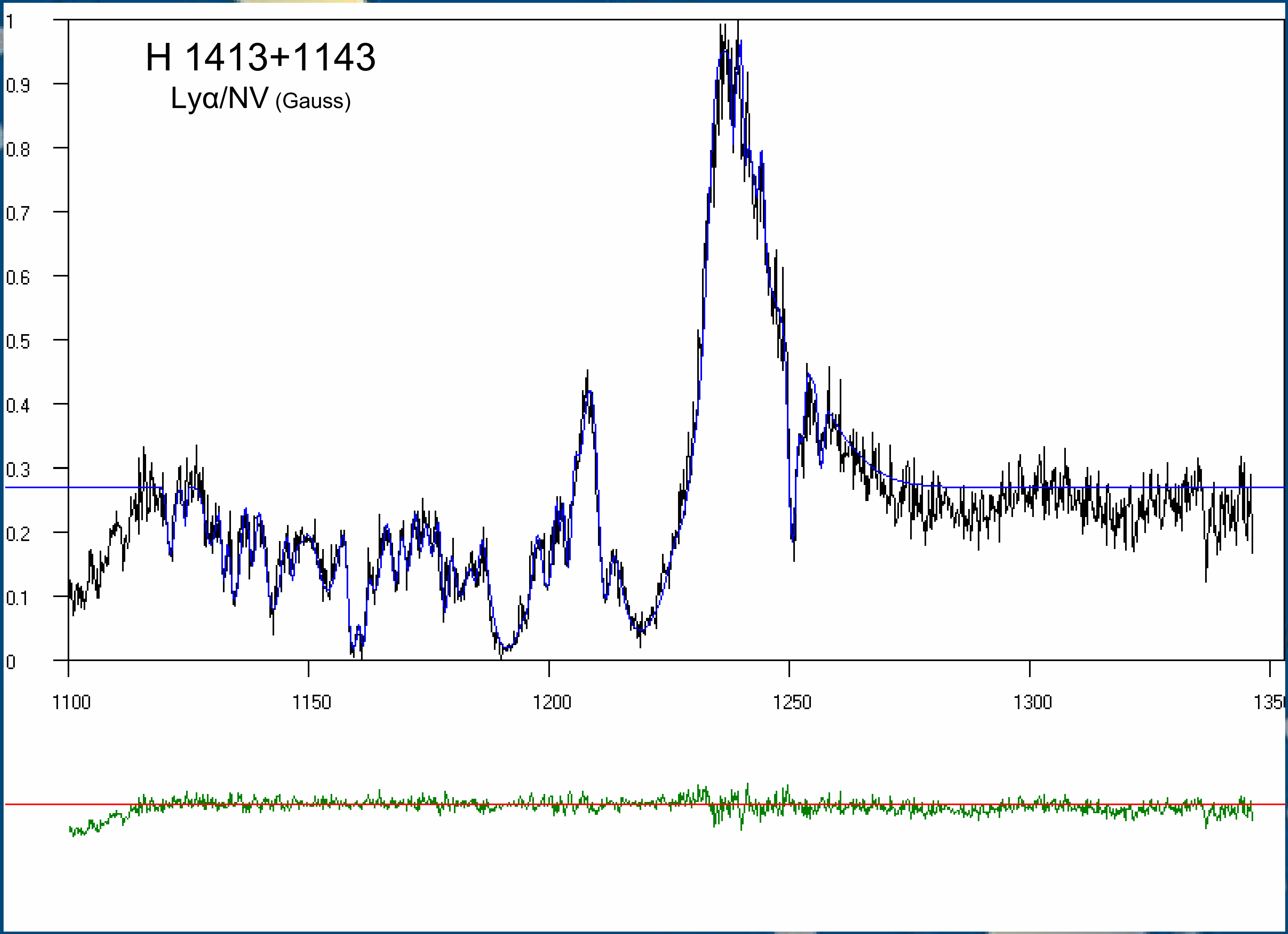

H 1413+1143
Lyα/NV (Gauss)
1
0.9
0.8
0.7
0.6
0.5
0.4
0.3
0.2
0.1
0
1100
1150
1200
1250
1300
135

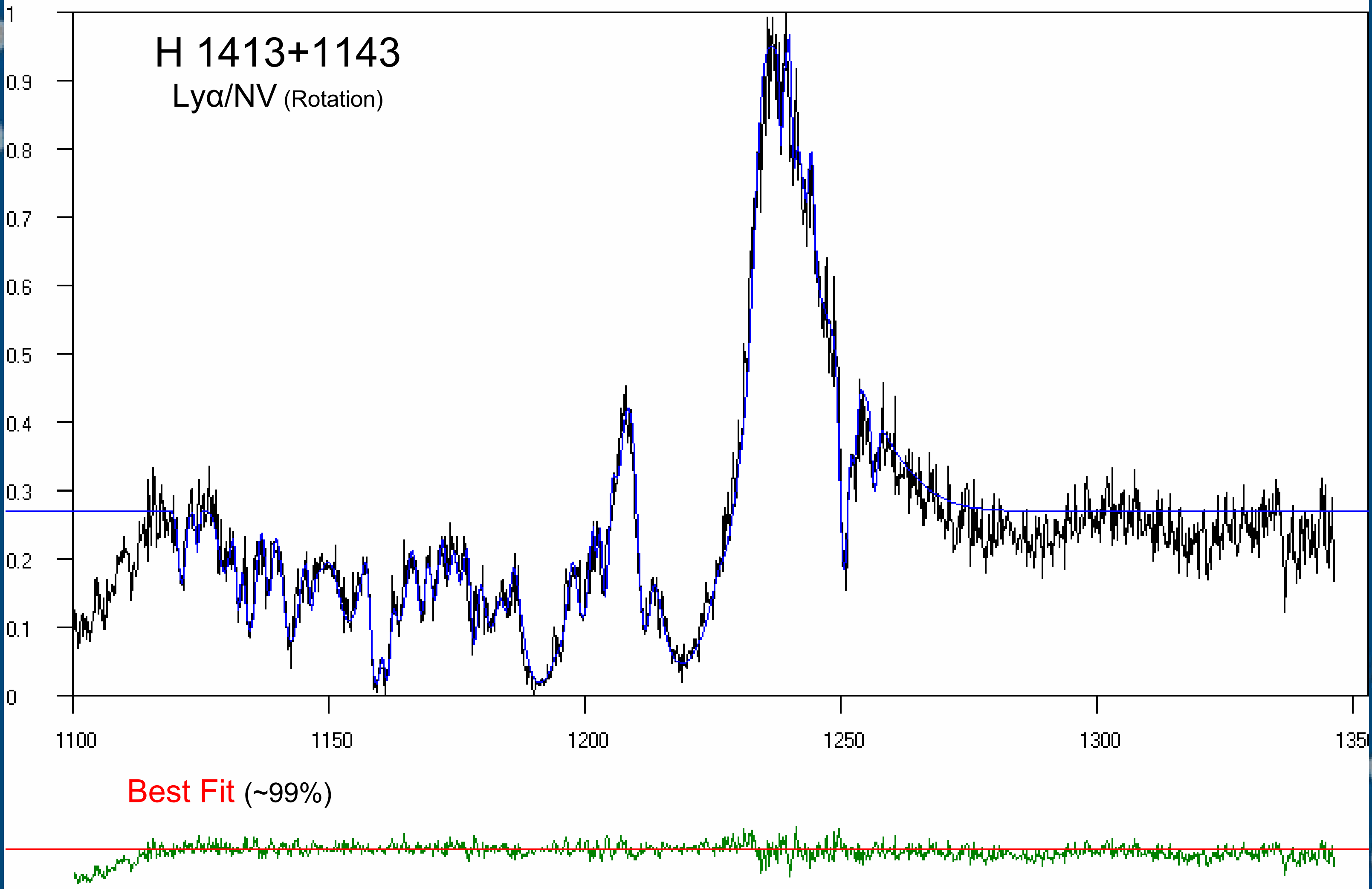

Lyα: 31 ALs up to -27000 km/s BALs up to -11000 km/s NV: 1 AL -3025 km/s

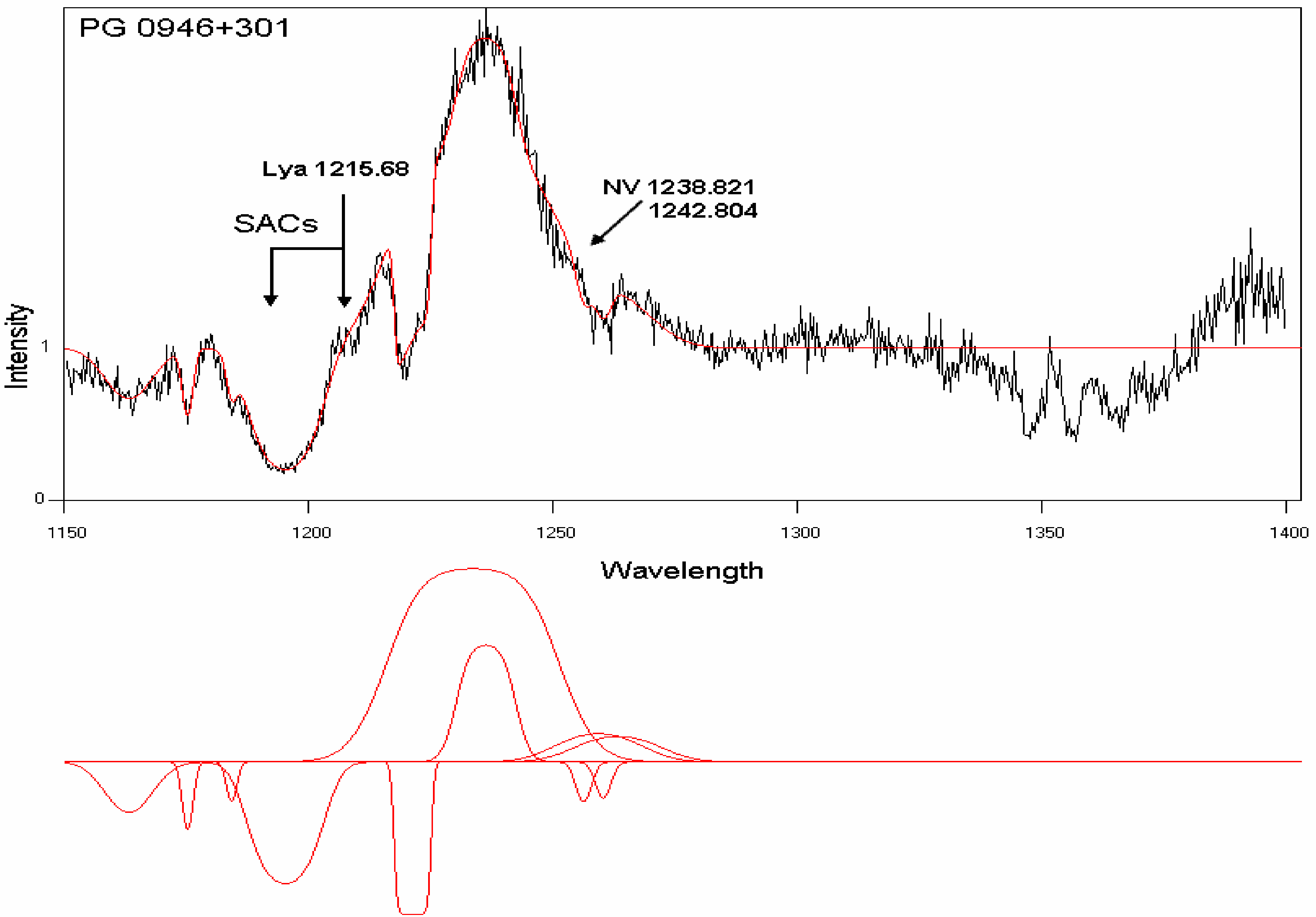
PG 0946+301
Lya 1215.68
SACs
NV 1238.821
1242.804
Intensity
1
0
1150
1200
1250
1300
1350
1400
Wavelength

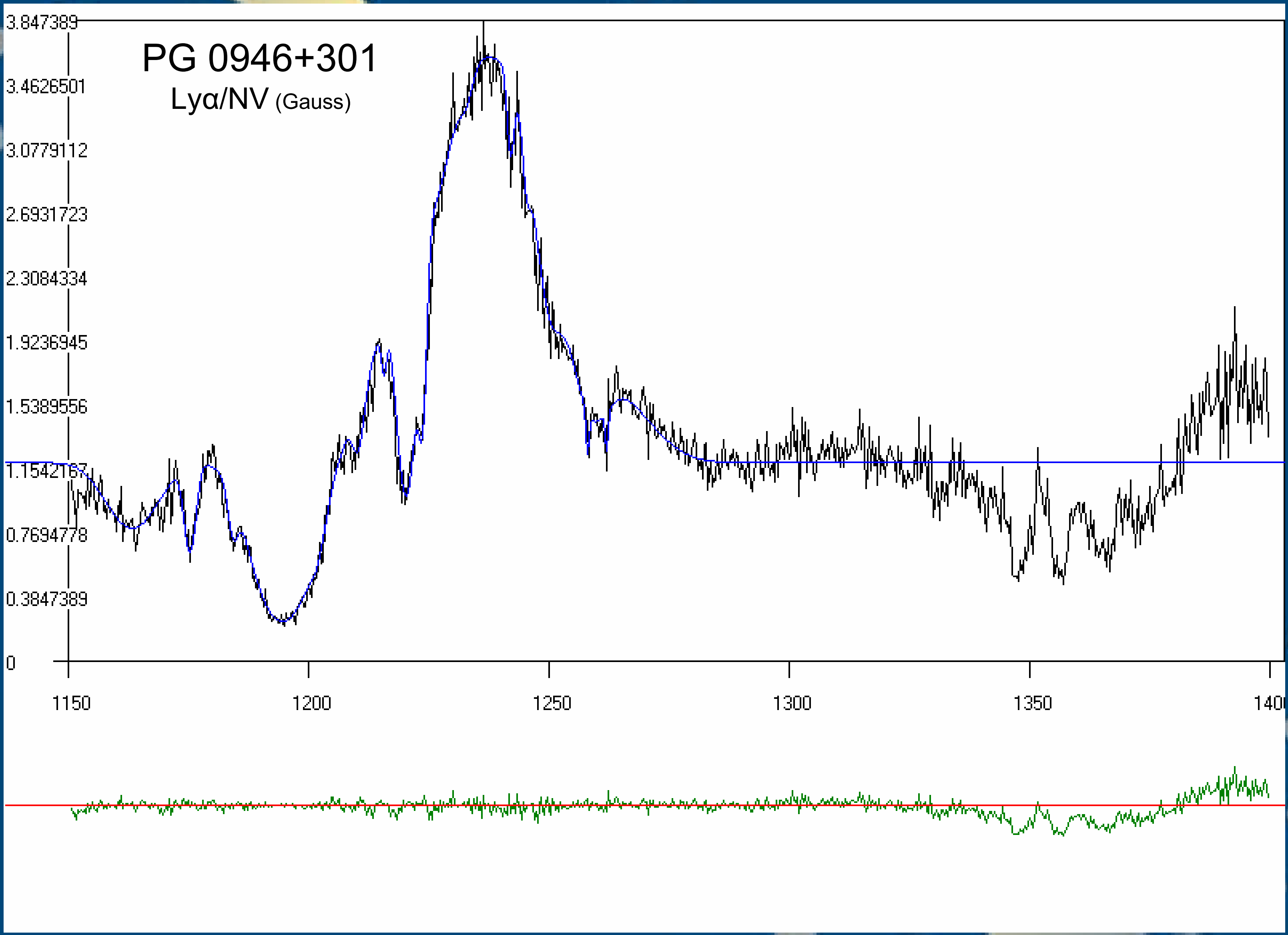

PG 0946+301
Lyα/NV (Gauss)
3.847389
3.4626501
3.0779112
2.6931723
2.3084334
1.9236945
1.5389556
1.1542167
0.7694778
0.3847389
0
1150
1200
1250
1300
1350
1400

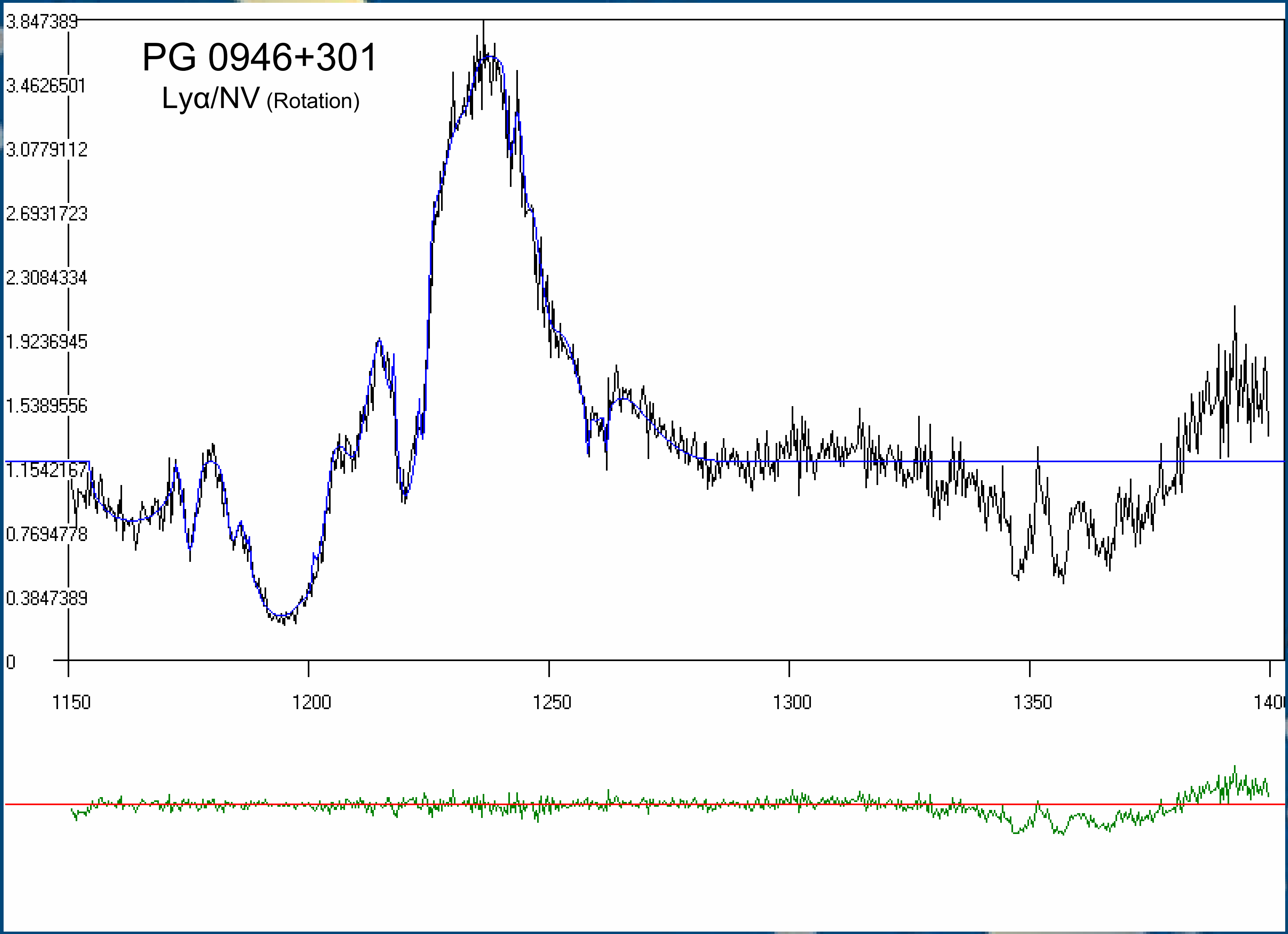
PG 0946+301
Lyα/NV (Rotation)
3.847389
3.4626501
3.0779112
2.6931723
2.3084334
1.9236945
1.5389556
1.1542167
0.7694778
0.3847389
0
1150
1200
1250
1300
1350
140

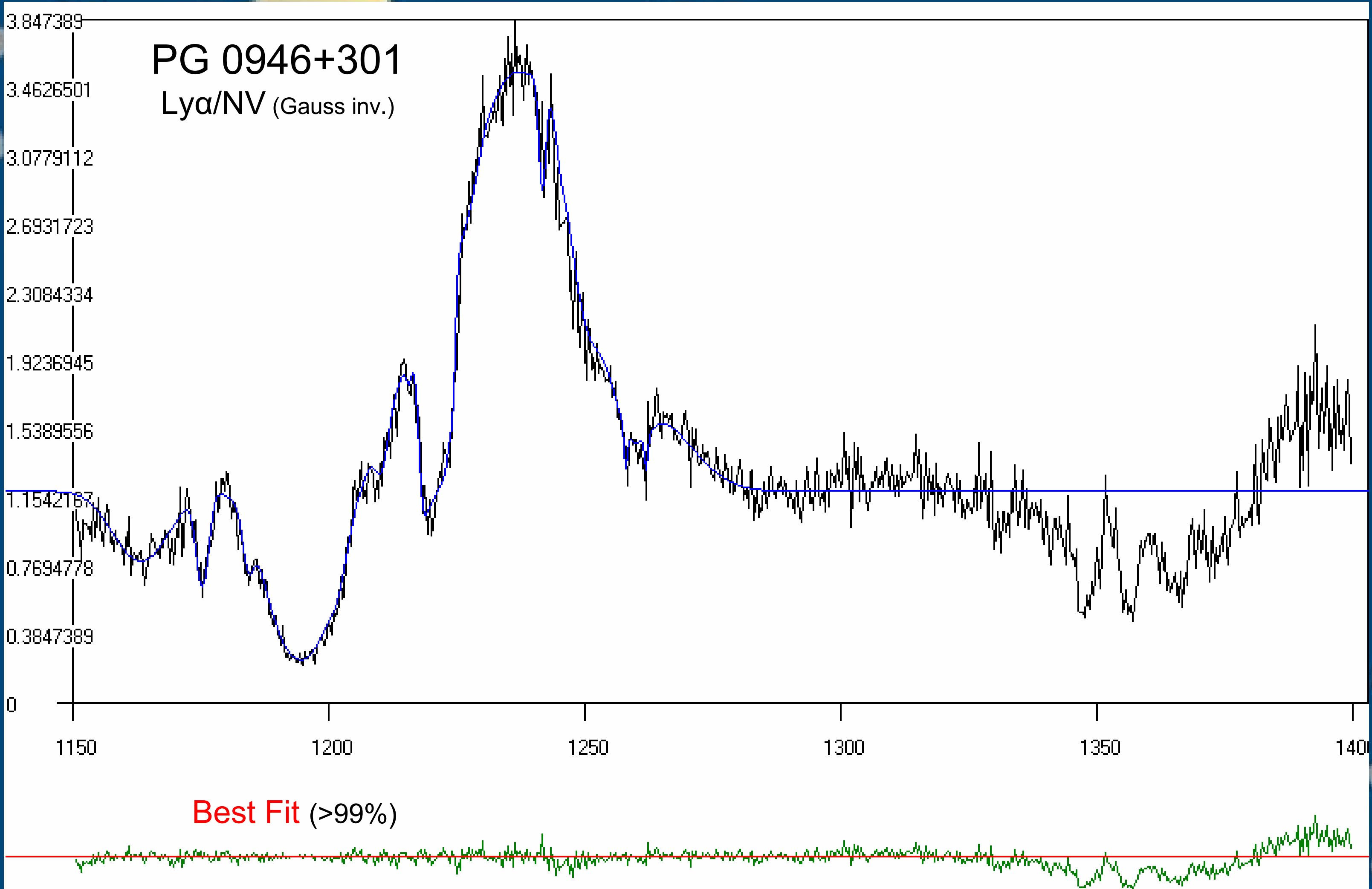

Lyα: 10 ALs up to -17260 km/s BALs up to -9500 km/s NV: 1 AL -340 km/s

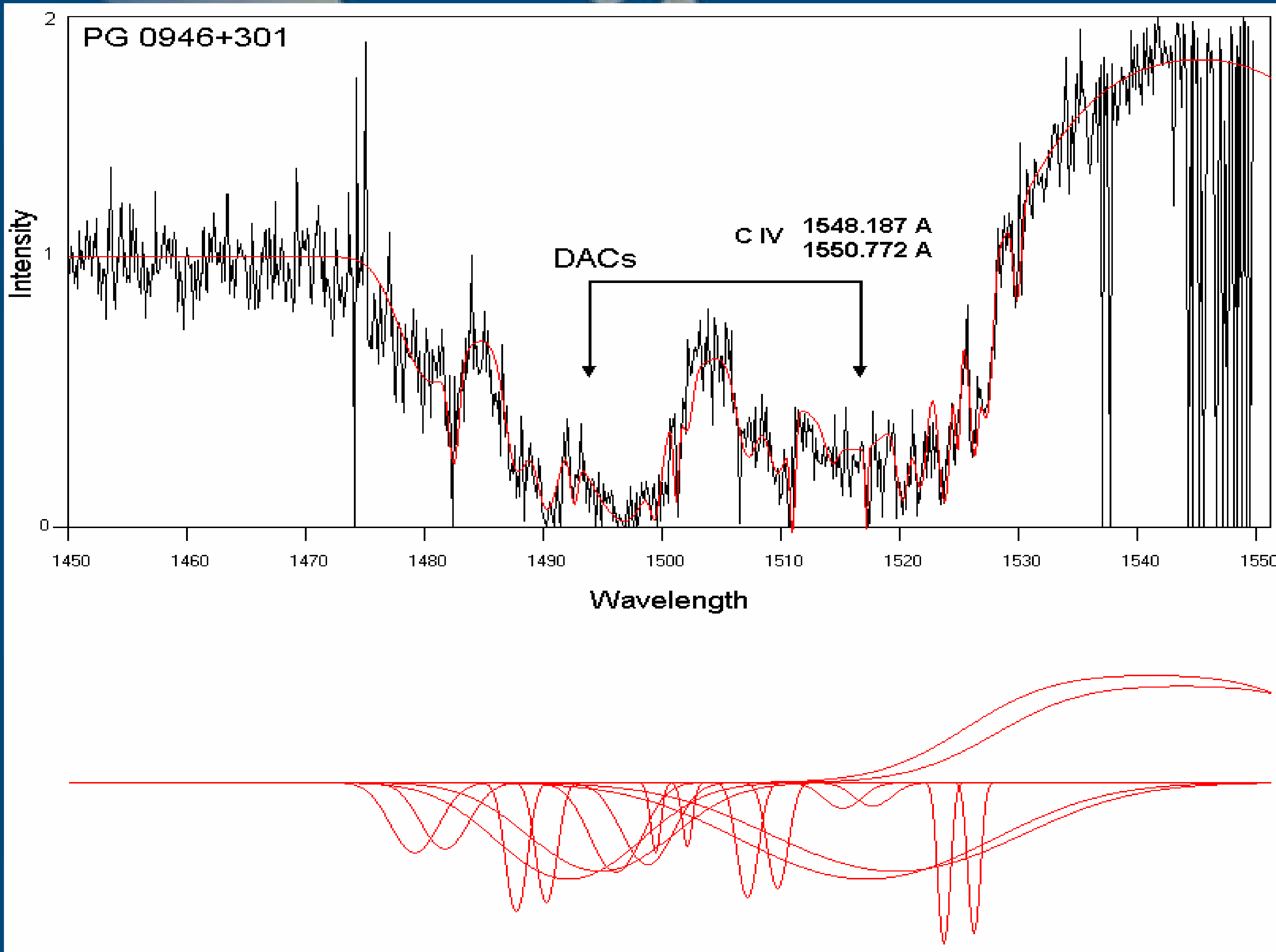
PG 0946+301
Intensity
Wavelength
DACs
C IV
1548.187 A
1550.772 A
0
1
2
1450
1460
1470
1480
1490
1500
1510
1520
1530
1540
1550

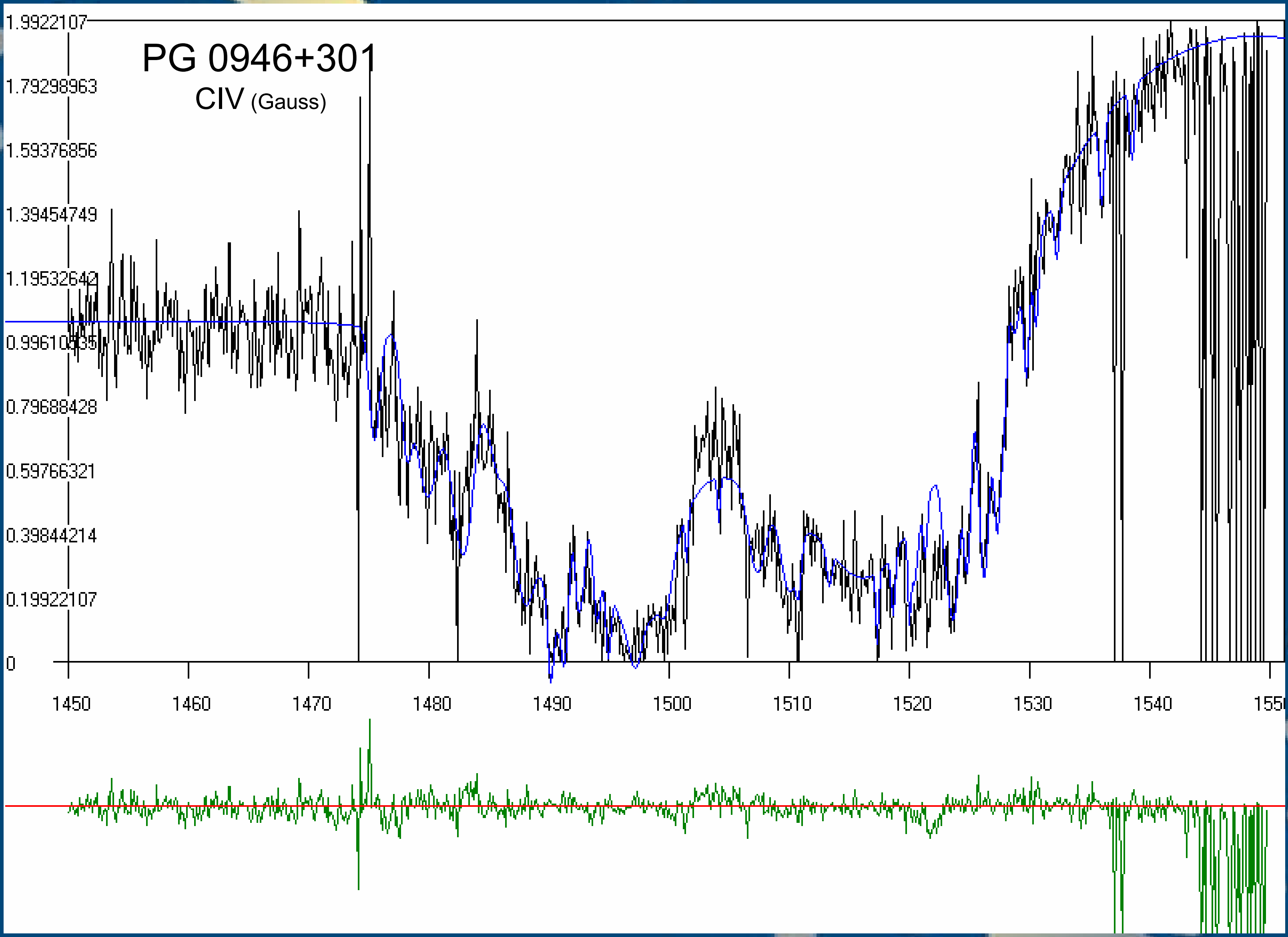
PG 0946+301
CIV (Gauss)
1.9922107
1.79298963
1.59376856
1.39454749
1.19532642
0.99610535
0.79688428
0.59766321
0.39844214
0.19922107
0
1450
1460
1470
1480
1490
1500
1510
1520
1530
1540
1550

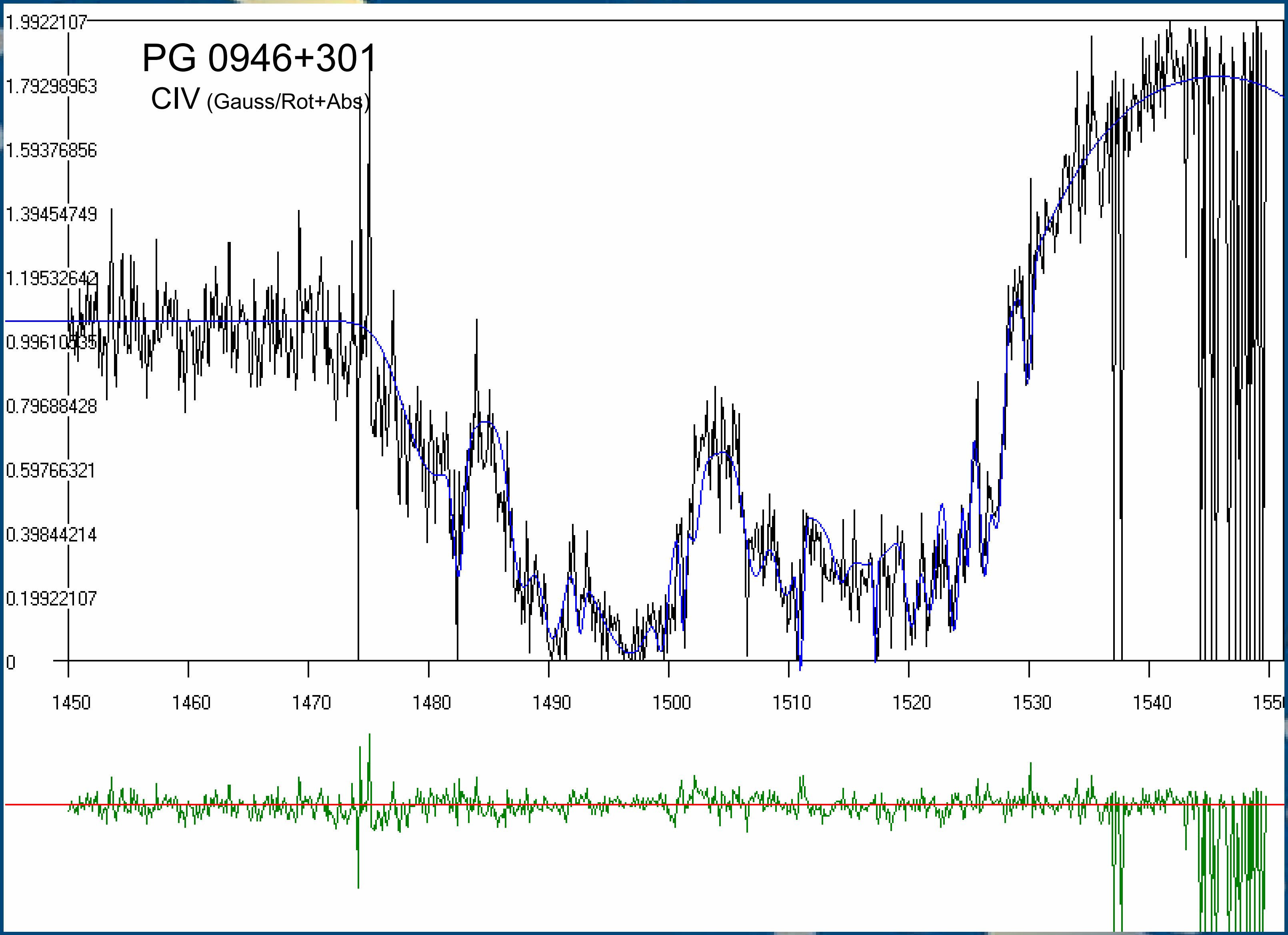

PG 0946+301
CIV (Gauss/Rot+Abs)
1.9922107
1.79298963
1.59376856
1.39454749
1.19532642
0.99610535
0.79688428
0.59766321
0.39844214
0.19922107
0
1450
1460
1470
1480
1490
1500
1510
1520
1530
1540

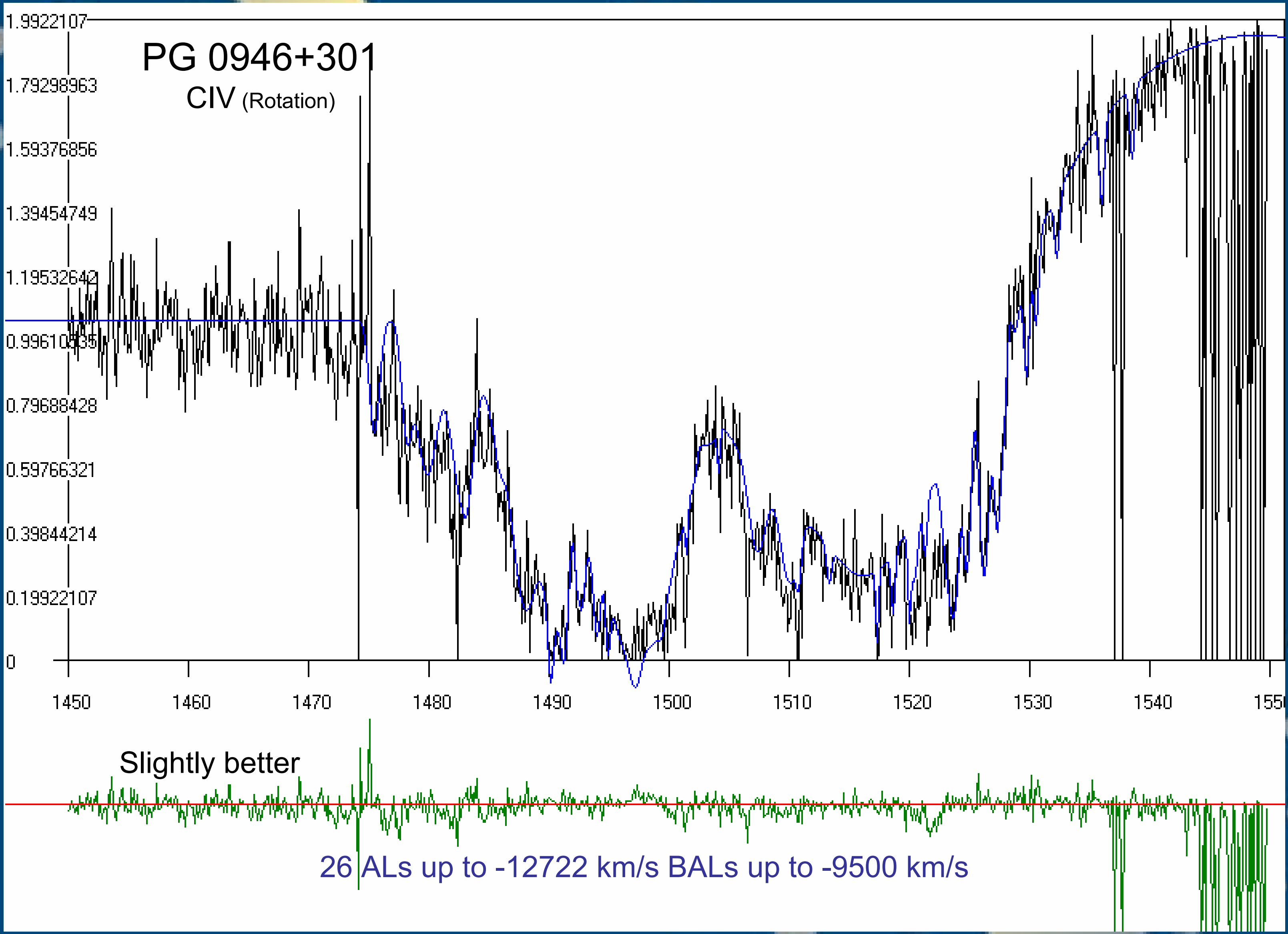

PG 0946+301
CIV (Rotation)
1.9922107
1.79298963
1.59376856
1.39454749
1.19532642
0.99610535
0.79688428
0.59766321
0.39844214
0.19922107
0
1450
1460
1470
1480
1490
1500
1510
1520
1530
1540
1550
Slightly better
26 ALs up to -12722 km/s BALs up to -9500 km/s

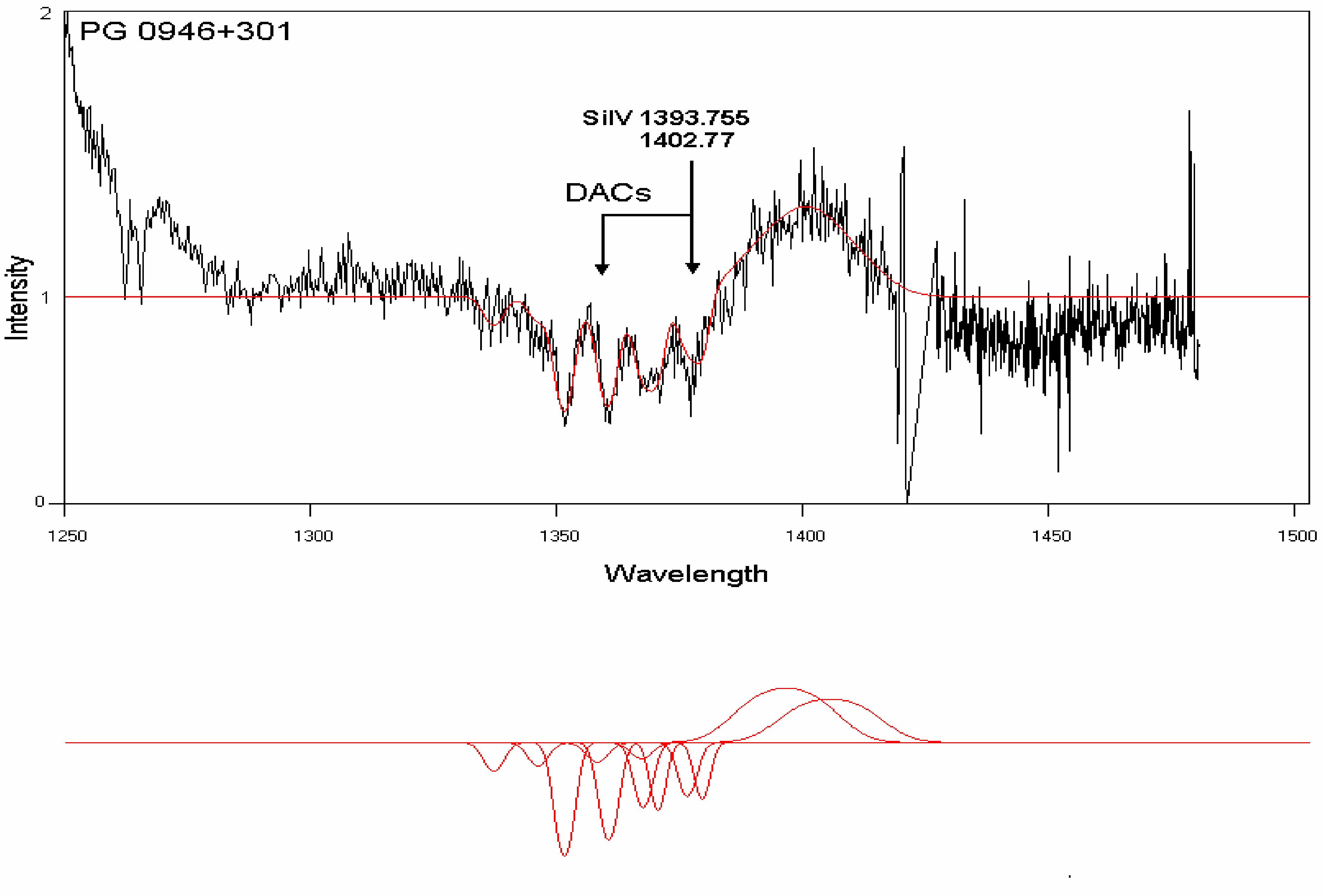

PG 0946+301
SiIV 1393.755
1402.77
DACs
Intensity
Wavelength
2
1
0
1250
1300
1350
1400
1450
1500

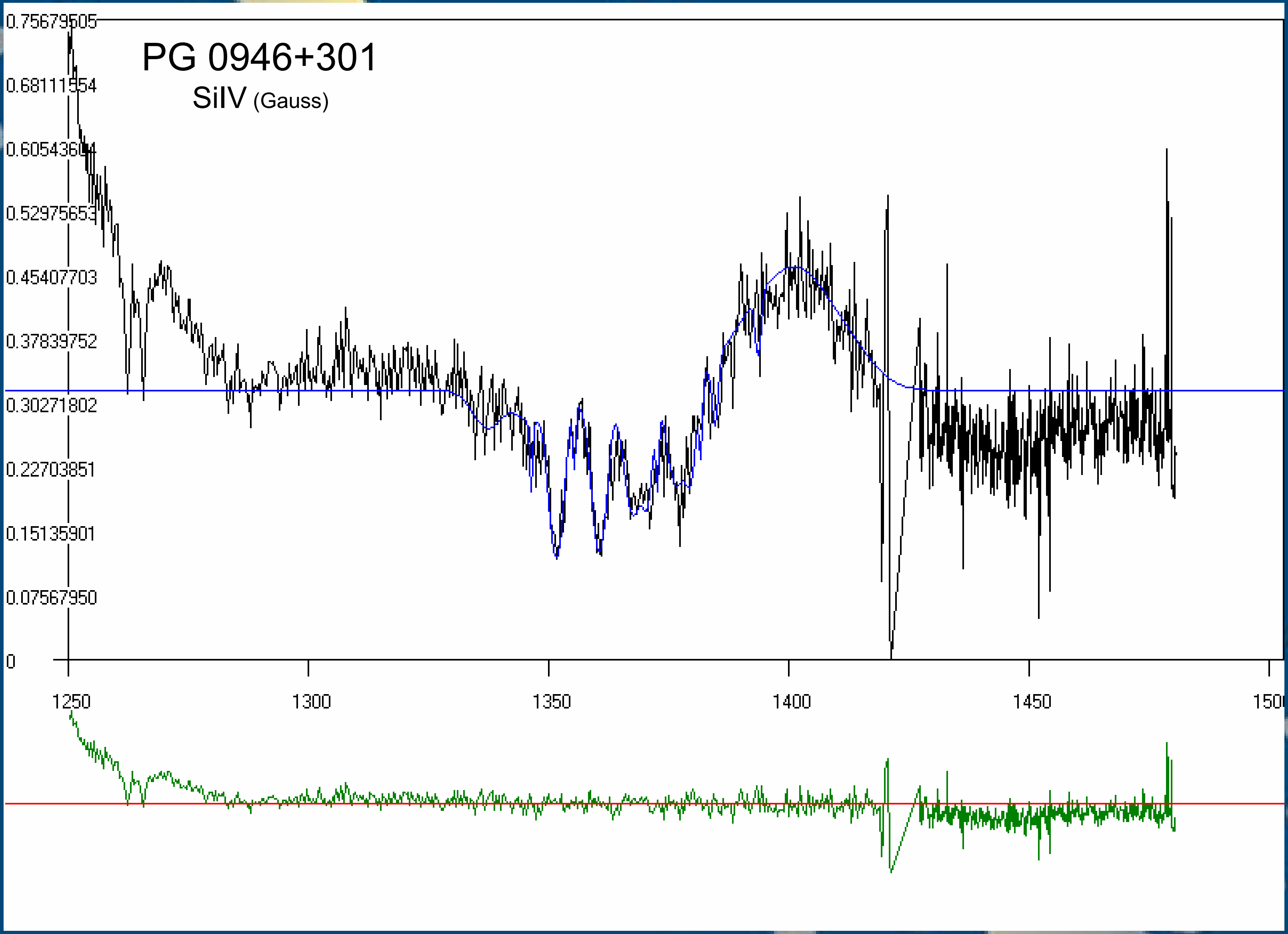

PG 0946+301
SiIV (Gauss)
0.75679505
0.68111554
0.60543604
0.52975653
0.45407703
0.37839752
0.30271802
0.22703851
0.15135901
0.07567950
0
1250
1300
1350
1400
1450
150

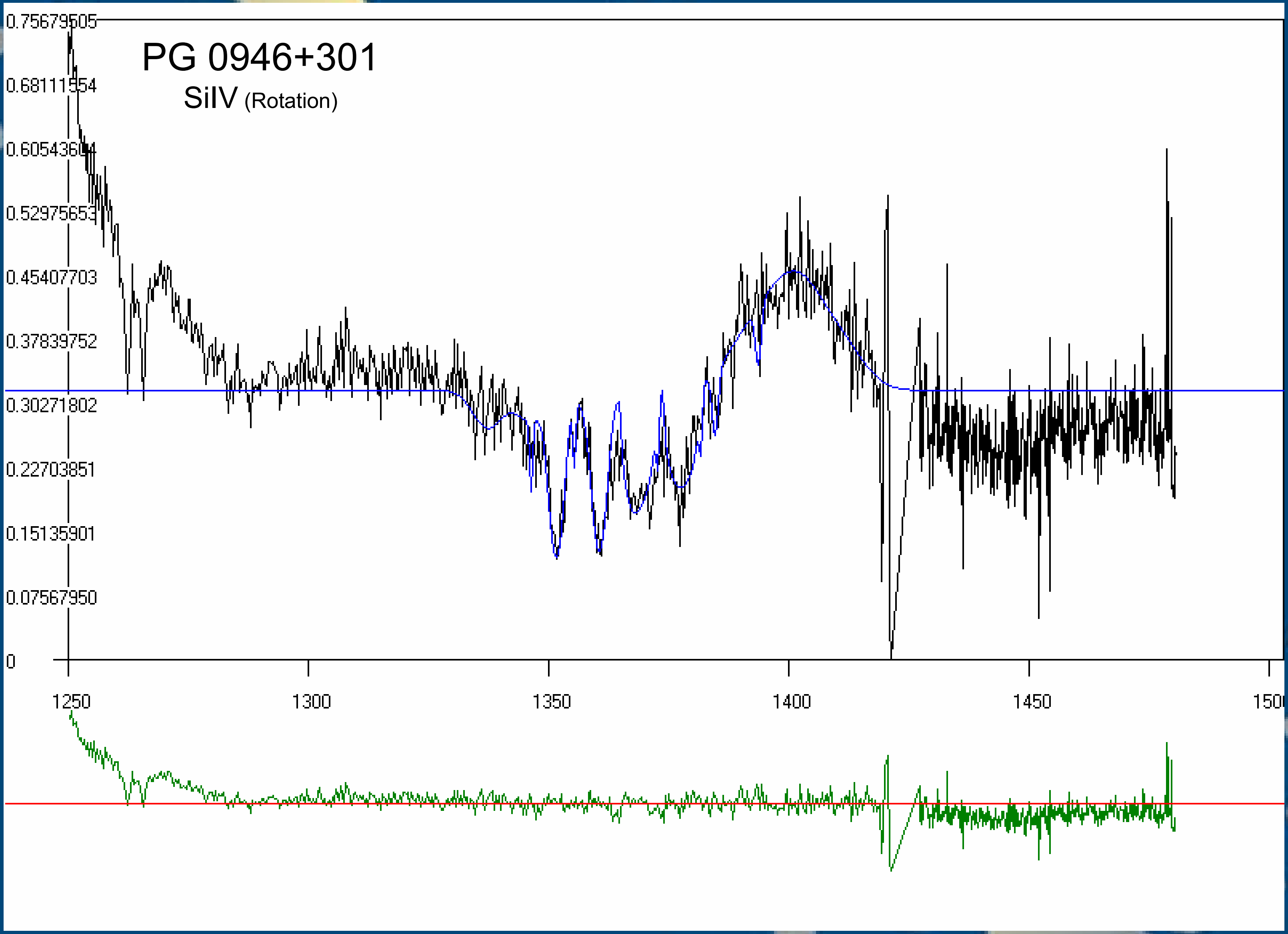
PG 0946+301
SiIV (Rotation)
0.75679505
0.68111554
0.60543604
0.52975653
0.45407703
0.37839752
0.30271802
0.22703851
0.15135901
0.07567950
0
1250
1300
1350
1400
1450
1500

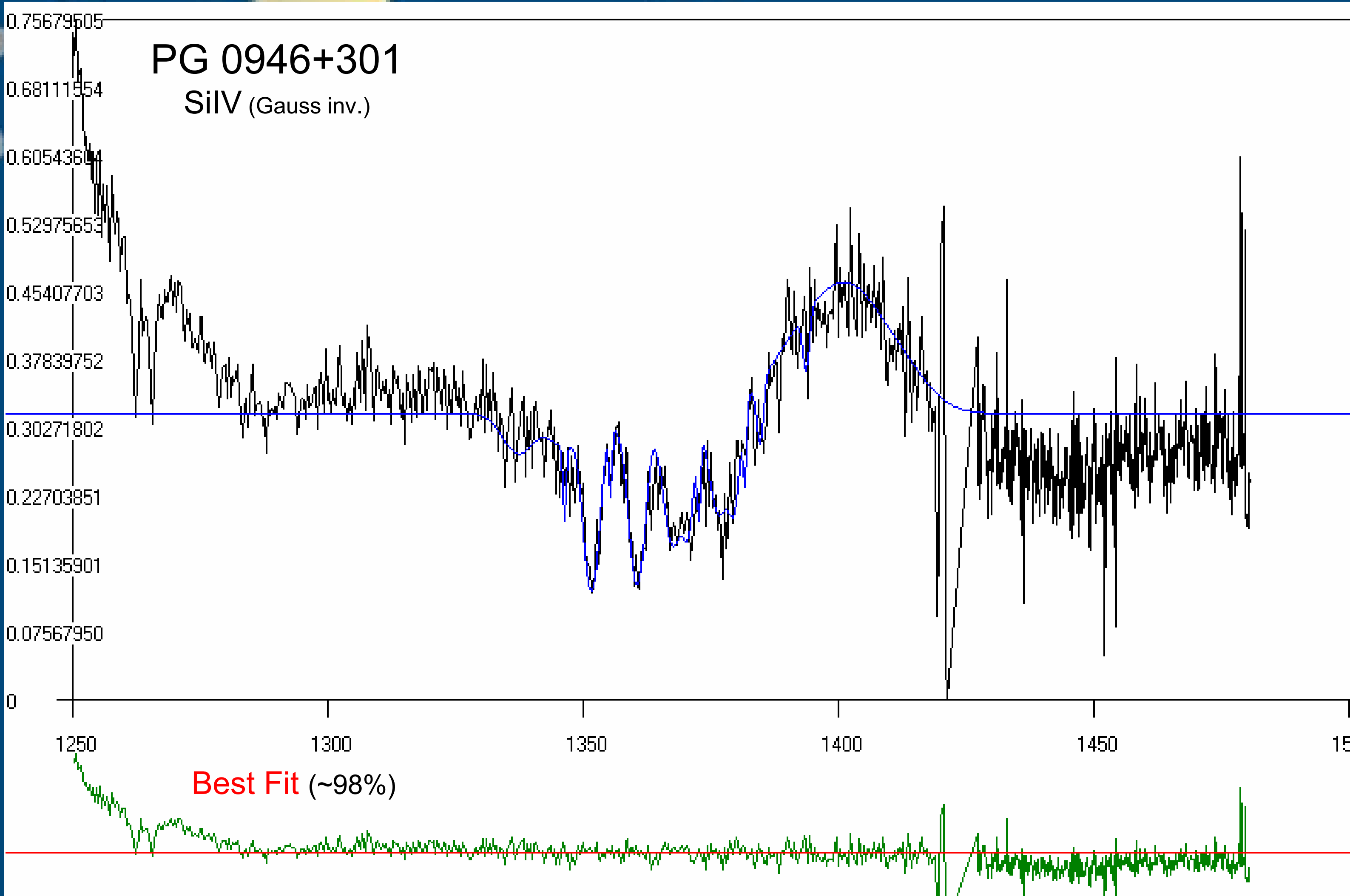

8 ALs up to -12755 km/s BALs up to -9500 Km/s

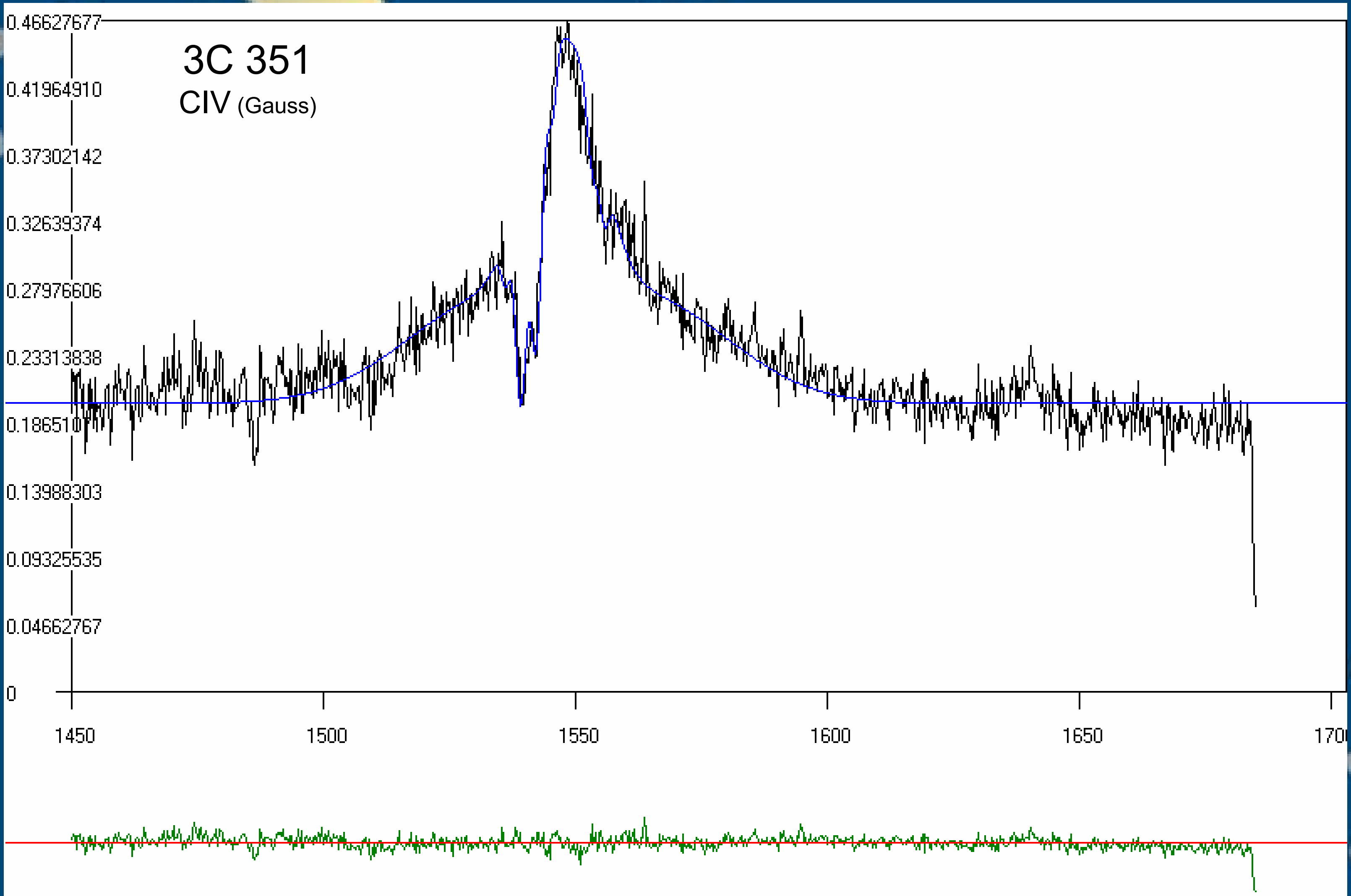

4 ALs up to -2130 km/s BALs up to -1720

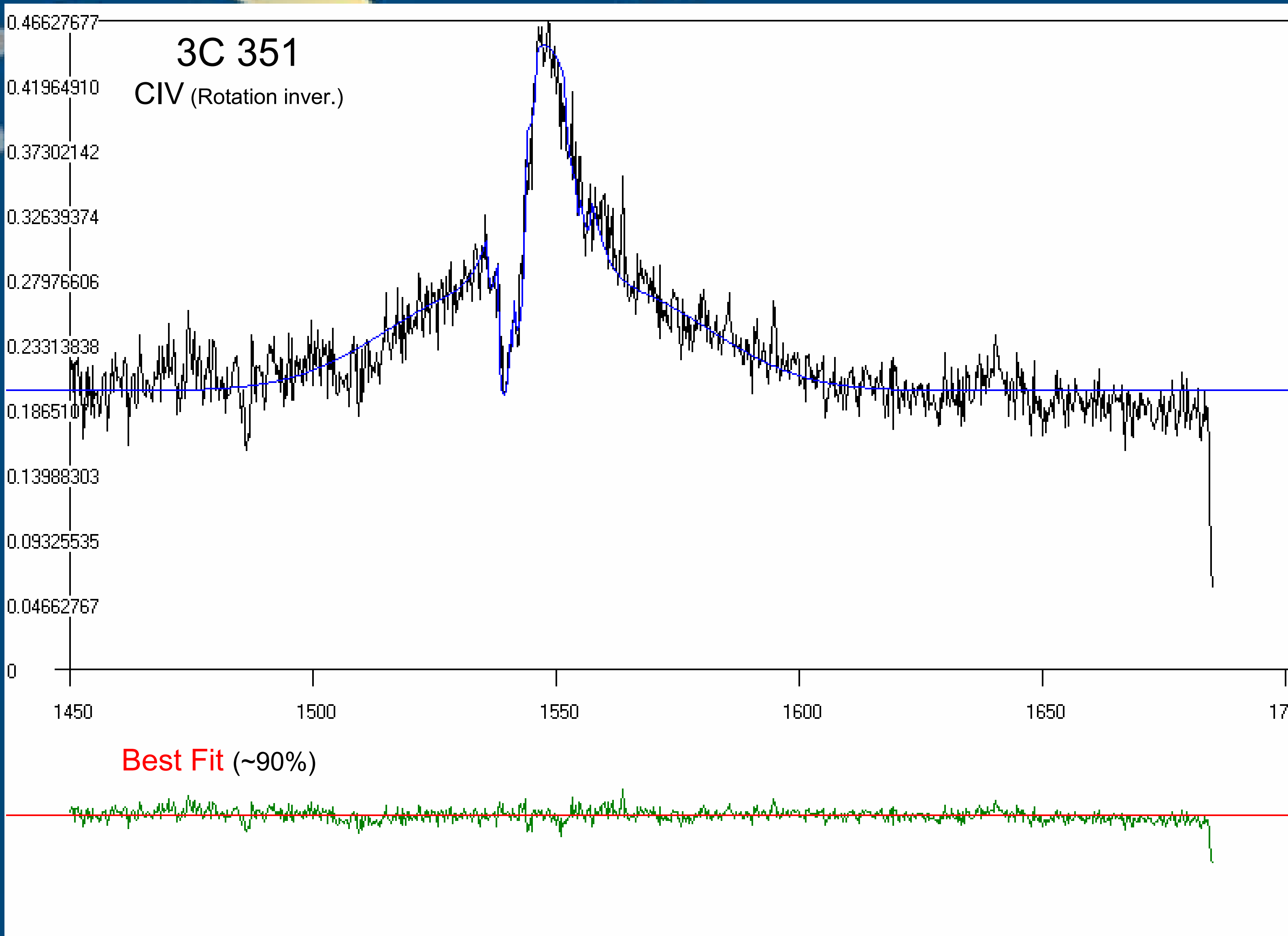
3C 351
CIV (Rotation inver.)
0.46627677
0.41964910
0.37302142
0.32639374
0.27976606
0.23313838
0.186510
0.13988303
0.09325535
0.04662767
0
1450
1500
1550
1600
1650
Best Fit (~90%)

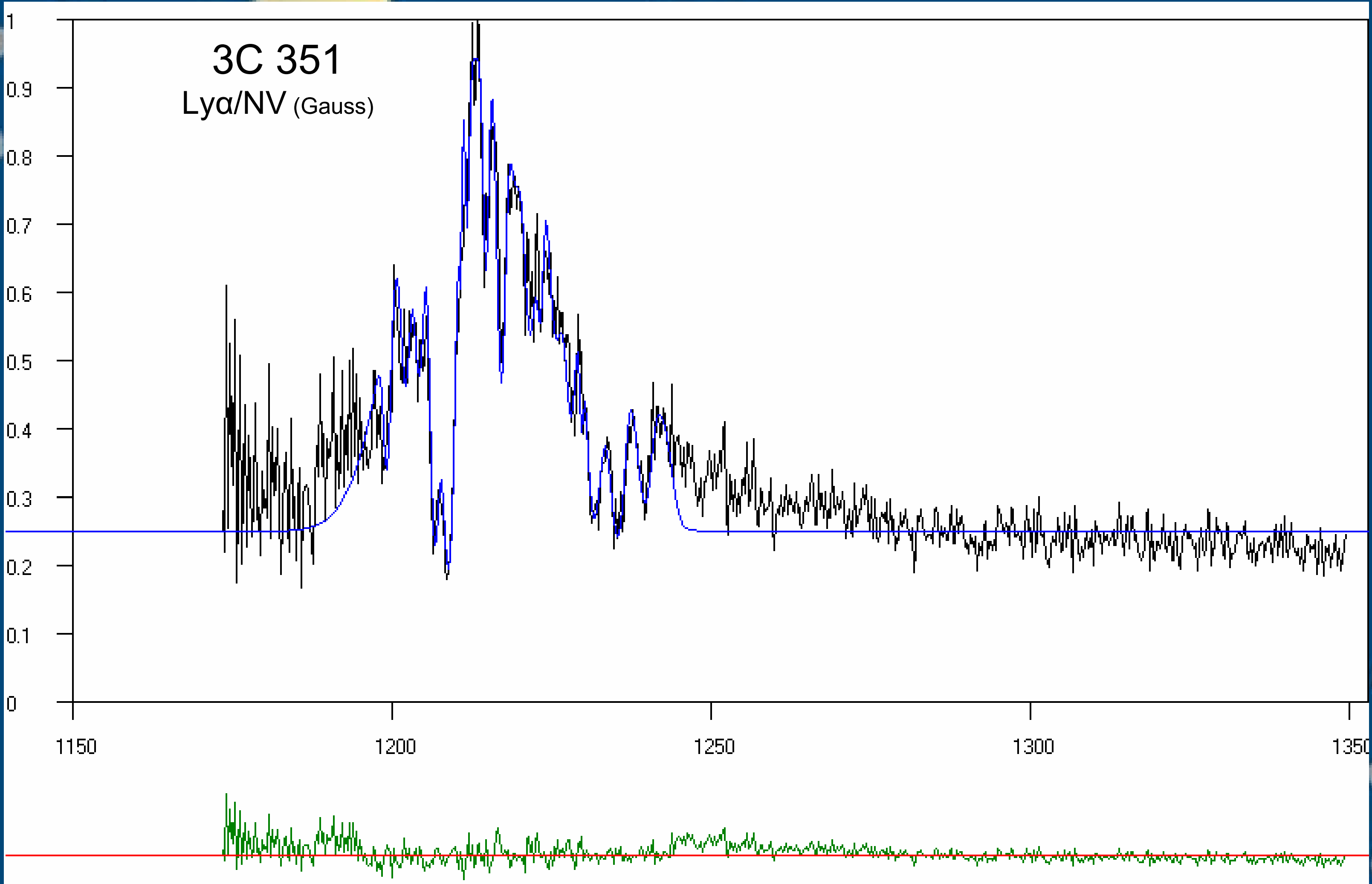

Lyα: 7 ALs up to -4070 km/s BALs up to -2200 NV: 1 AL -580 km/s

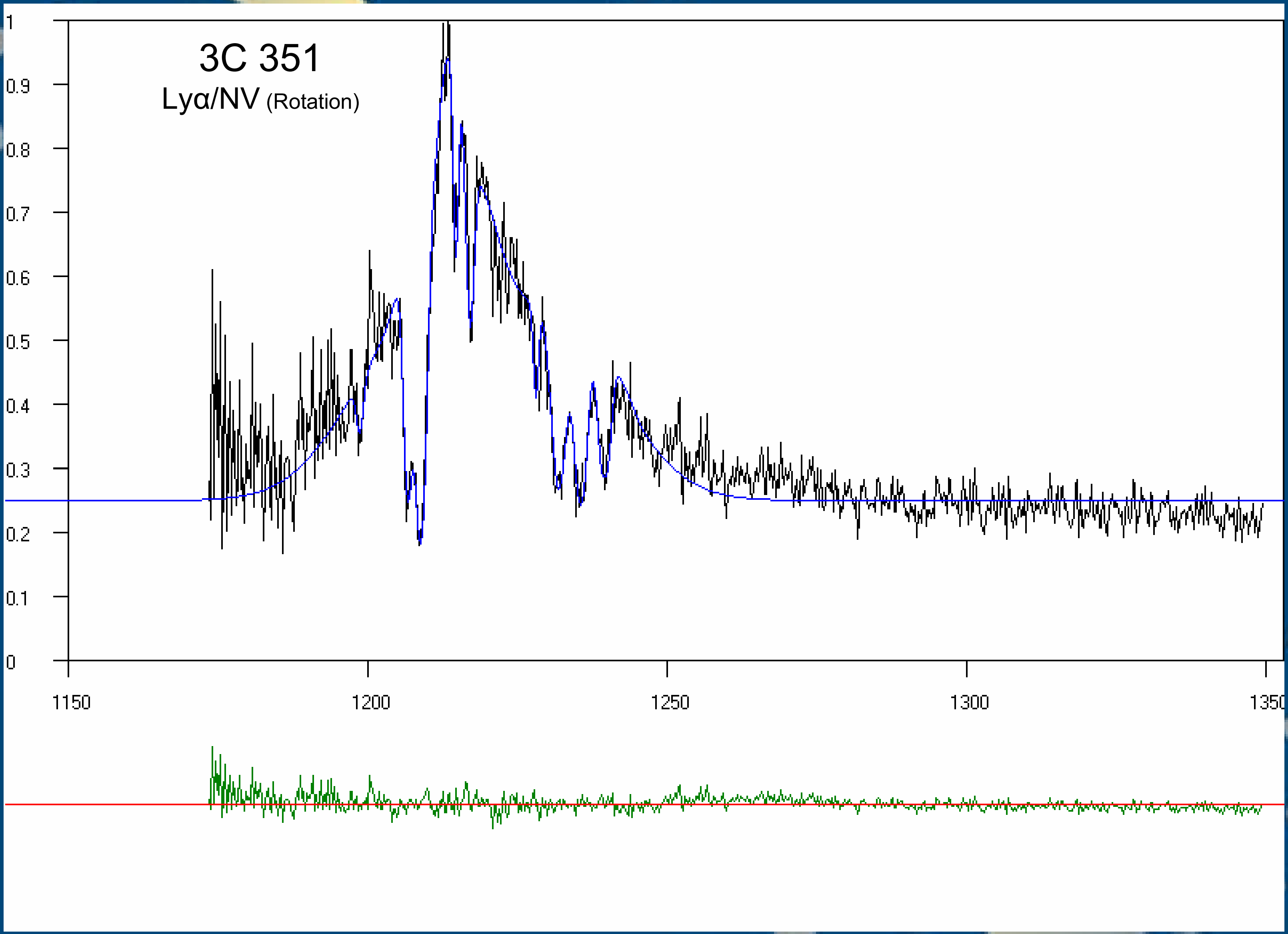
3C 351
Lyα/NV (Rotation)
1
0.9
0.8
0.7
0.6
0.5
0.4
0.3
0.2
0.1
0
1150
1200
1250
1300
1350

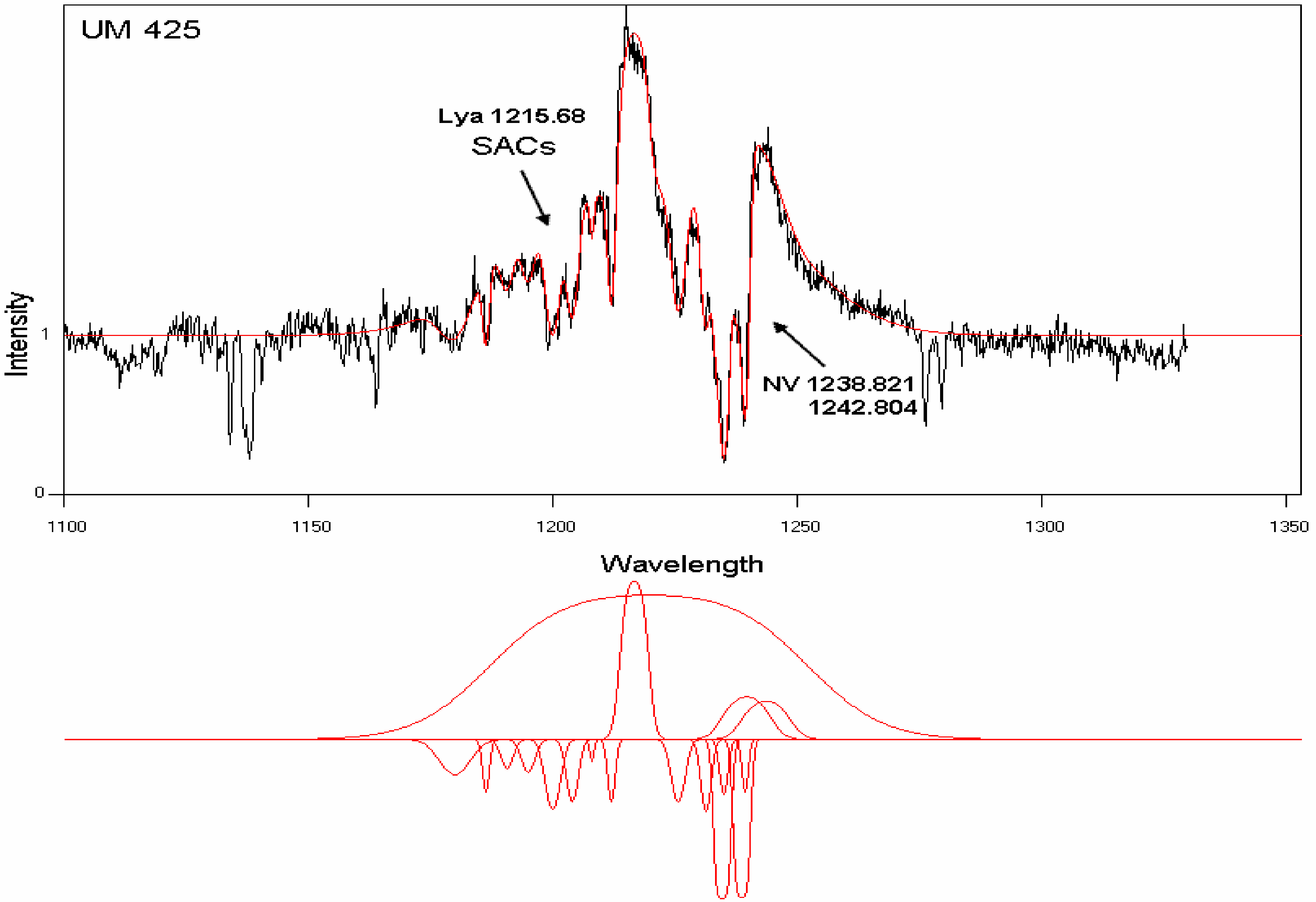

UM 425
Lya 1215.68
SACs
NV 1238.821
1242.804
Intensity
1
0
1100
1150
1200
1250
1300
1350
Wavelength

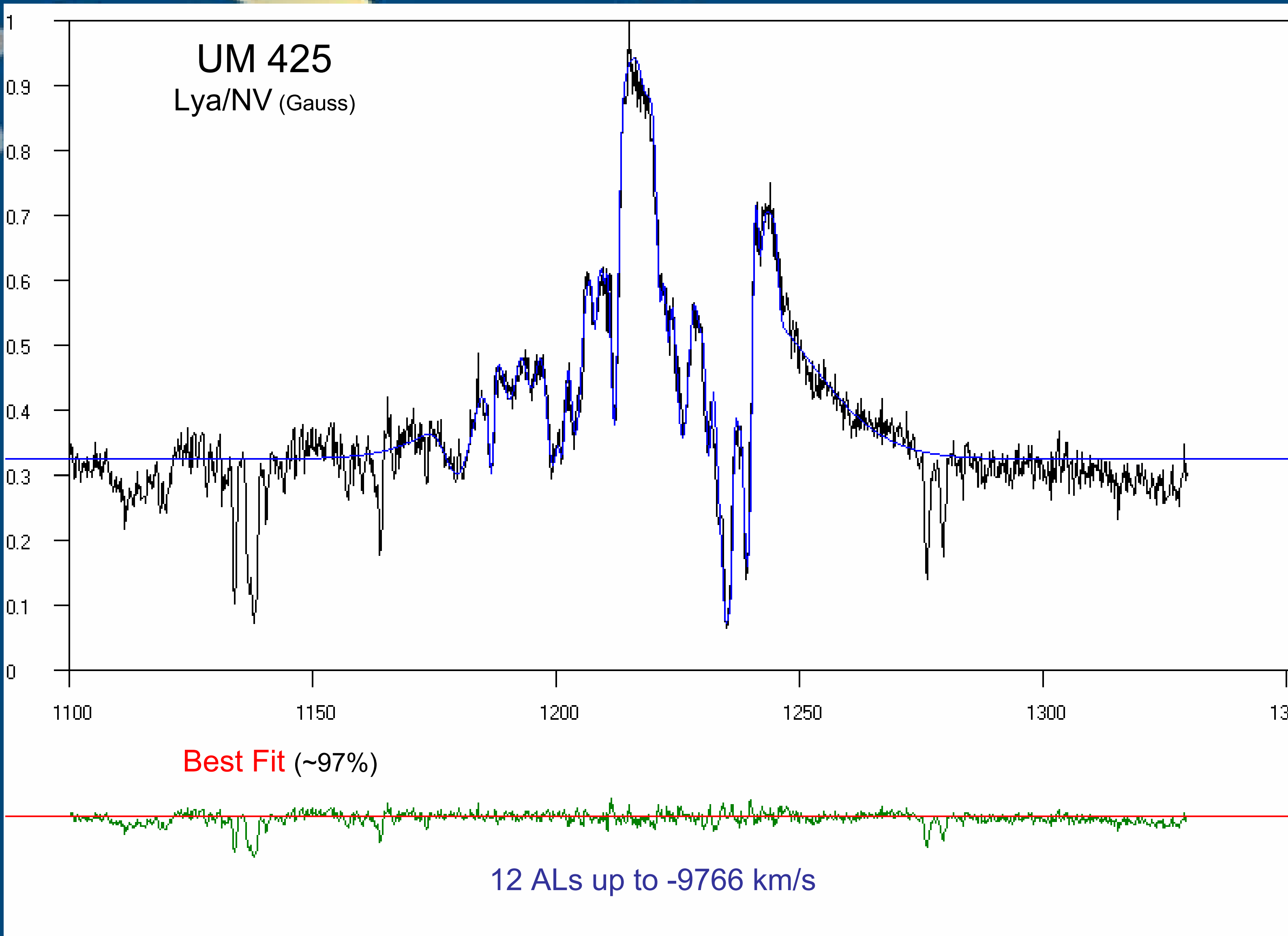
UM 425
Lya/NV (Gauss)
1
0.9
0.8
0.7
0.6
0.5
0.4
0.3
0.2
0.1
0
1100
1150
1200
1250
1300
1350
Best Fit (~97%)
12 ALs up to -9766 km/s

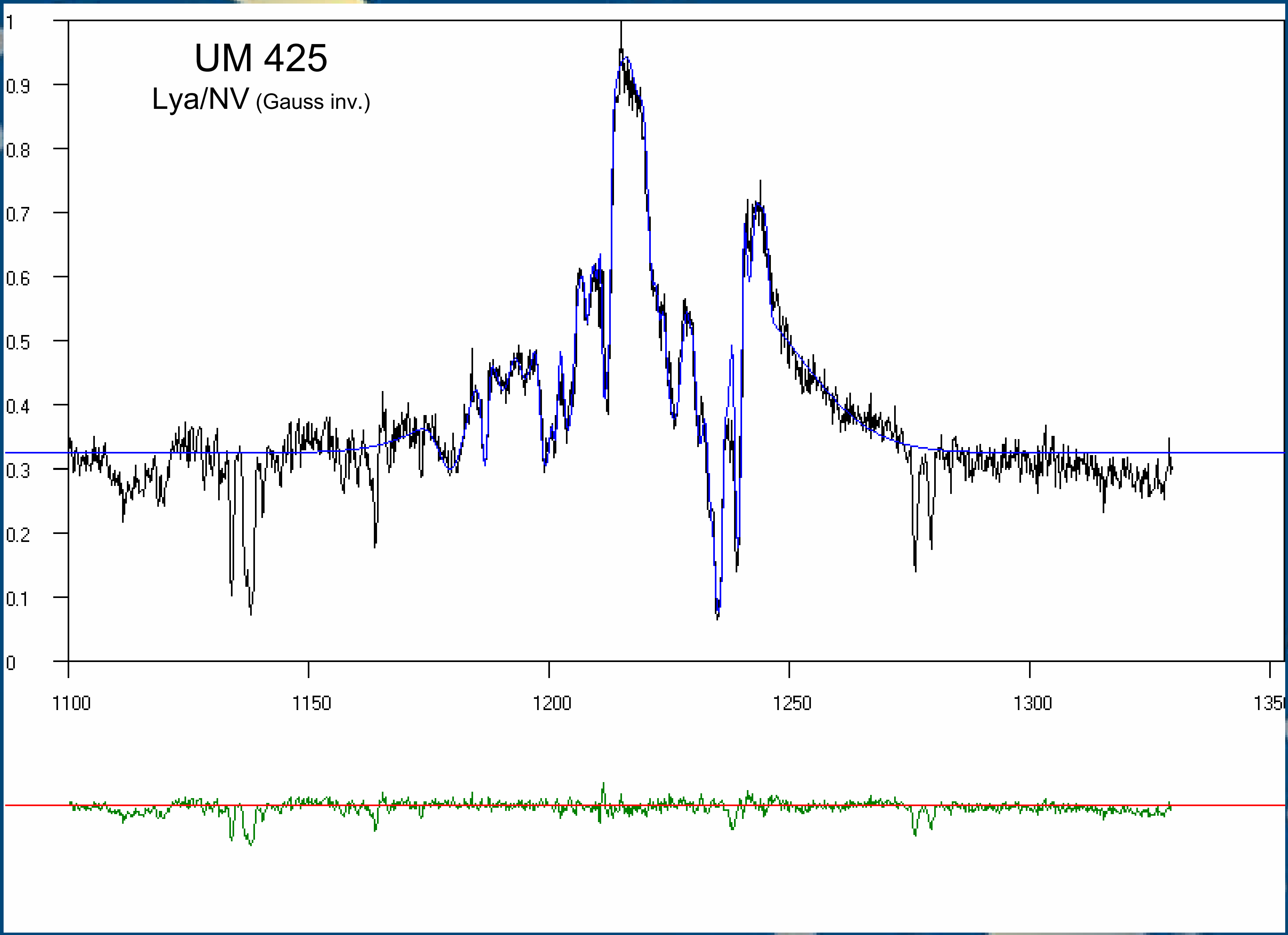

UM 425
Lya/NV (Gauss inv.)
1
0.9
0.8
0.7
0.6
0.5
0.4
0.3
0.2
0.1
0
1100
1150
1200
1250
1300
1350

CONCLUSIONS

No unique solution – rather a range of parameters for the absorbing flow.

What we intended here is to demonstrate that it is possible to describe the complex BAL QSO profiles with a relatively simple model.

Large sample of high S/N spetra of BAL QSOs, to draw statistically significant conclusions.

Adjustment of the model (e.g. include random *and* rotational velocities), search for Lyα “ghost” signatures, etc.

Extract various parameters (asymmetry, line shape, optical depth, flux ratios, etc).

T	L	Vrot ΔL	Voigt Mix	Xi	Semit	Tau	ΔL	W.Length	FWHM	Vr	Vrand		Col.Deni	Ei
E	G	20.000		2.200	.050	.110	-1.000	1548.187	64.977	-193.6413	4563.054000	2.927638	1.902330E+10	8.008350
E	G	5.500		1.400	.115	.161	-2.000	1548.187	16.209	-387.2826	1254.840000	1.438782	9.348966E+09	8.008350
A	G	.980		.620			-8.900	1548.187	2.569	-1723.407	223.589600	-2.477427E-01	-1.609791E+09	8.008350
A	G	.950		.170			-5.800	1548.187	2.306	-1123.119	216.745000	-7.631493E-02	-4.958818E+08	8.008350
A	G	.950		.170			5.000	1548.187	2.306	968.206	216.745000	-7.631493E-02	-4.958818E+08	8.008350
A	G	.900		.150			-12.000	1548.187	2.177	-2323.695	205.337400	-6.423164E-02	-4.173665E+08	8.008350
A	G	.600		.050			-5.000	1548.187	1.426	-968.206	136.891600	-1.477748E-02	-9.602162E+07	8.008350